PREPARED FOR THE U.S. DEPARTMENT OF ENERGY,
UNDER CONTRACT DE-AC02-76-CHO-3073

**PPPL-3041**
UC-427

**PPPL-3041**

# QUASILINEAR ANALYSIS OF ABSORPTION OF ION BERNSTEIN WAVES BY ELECTRONS

BY

A. CARDINALI, F. PAOLETTI, S. BERNABEI AND M. ONO

JANUARY 1995

PPPL PRINCETON PLASMA PHYSICS LABORATORY



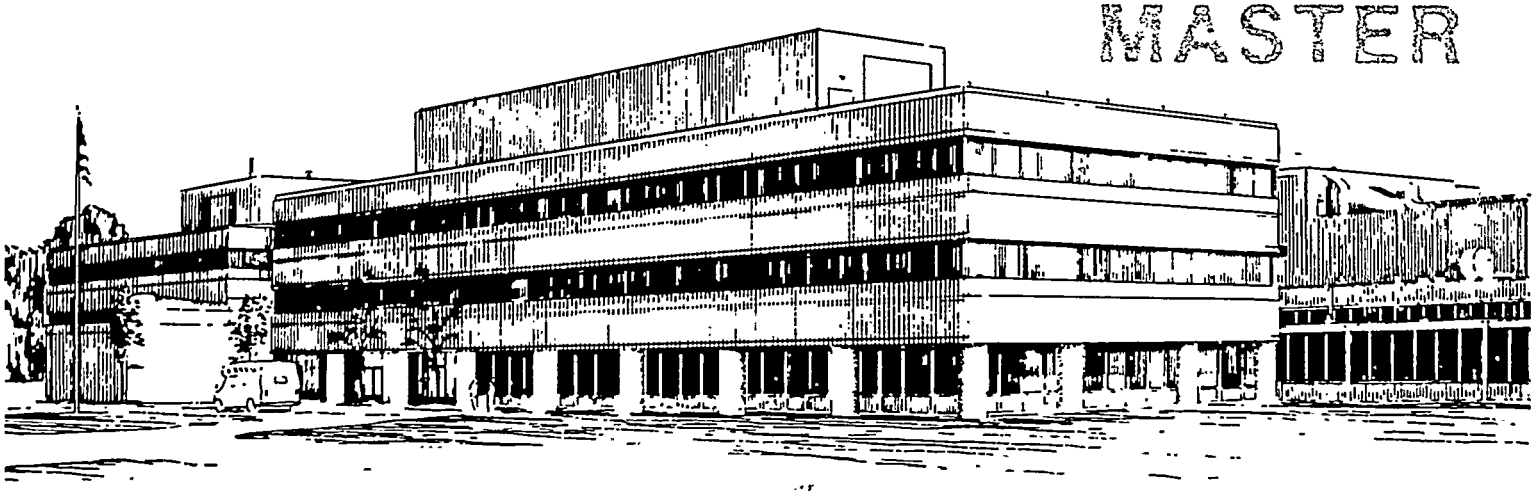

PRINCETON UNIVERSITY, PRINCETON, NEW JERSEY

## NOTICE

# QUASILINEAR ANALYSIS OF ABSORPTION OF ION BERNSTEIN WAVES BY ELECTRONS

A. Cardinali*, F. Paoletti^, S. Bernabei+, M. Ono+

*Associazione Euratom-ENEA sulla Fusione, Centro Ricerche Energia Frascati, C.P. 65, 00044 Frascati, Rome, Italy

+Princeton University, Plasma Physics Laboratory, Forrestal Campus, P.O. Box 451, Princeton, New Jersey 08543

^Massachusetts Institute of Technology, 77 Massachusetts Avenue, Cambridge, Massachusetts 02139

## ABSTRACT

The effects induced on plasma electrons by an externally launched ion Bernstein wave (IBW), in the presence of a lower hybrid wave (LHW) in the current drive regime, are studied by analytical integration of the IBW ray-tracing equations along with the amplitude transport equation (Poynting theorem). The electric field amplitude parallel and perpendicular to the external magnetic field, the quasilinear diffusion coefficient, and the modified electron distribution function are analytically calculated in the case of IBW. The analytical calculation is compared to the numerical solution obtained by using a 2-D Fokker-Planck code for the distribution function, without any approximation for the collision operator. The synergy between the IBW and LHW can be accounted for, and the absorption of the IBW power when the electron distribution function presents a tail generated by the LHW in the current drive regime can be calculated.

## I. INTRODUCTION

It has been shown[1,2,3] that the ion Bernstein wave, normally used to heat the bulk ions of the plasma at a given harmonic resonance, could also be used to heat the electron population directly due to the sharp increase of the parallel refraction index $n_{||}$ along the ray trajectory.

As previously shown,[2,3] $n_{||}$ oscillates along the trajectory, assuming both positive and negative values. Its amplitude depends essentially on the poloidal location of the antenna, and (when the antenna lies on the equatorial plane) on the $n_{||}$-spectrum launched by the antenna itself. Hence, a wide range of values of $n_{||}$ are present inside the plasma.

The IBW can be used in conjunction with the lower hybrid wave to improve the efficiency of lower hybrid current drive (LHCD).[4,5] This synergistic mechanism has been utilized by A. Ram, A. Bers and V. Fuchs[6] to explain the experimental results of LHCD on the Joint European Torus (JET),[7] where LHCD was used in conjunction with the ion cyclotron fast wave (ICFW) to improve current drive efficiency in the center of the plasma.

IBW alone normally cannot produce a net current in the plasma, because the launched wave spectrum changes continuously from positive to negative values. However, LHW launched with a spectrum centered on low values of $n_{||}$, lying just above the accessibility condition, generates an asymmetric tail in the electron distribution function that extends up to very low parallel velocities and produces a net current inside the plasma. The effect of IBW used in conjunction with LHCD can be twofold. First, IBW can sustain this current,

dissipating its energy on the side of the parallel velocity where the asymmetric tail already exists due to LHCD. Second, IBW can modify the distribution function of the electrons by helping to fill the so-called LHCD spectral gap for very low parallel velocity (high values of $n_{||}$). It is clear that the presence of the electric field due to IBW may modify the electron distribution function only if the amount of power, which flows parallel to the toroidal magnetic field, is sufficient to compensate for the collisional diffusion effects, which tend to restore the distribution function to a Maxwellian function. The relevant parameter is the ratio of the quasilinear diffusion coefficient to the collisional diffusivity, which measures the ability for IBW to extract the thermal electrons from the bulk distribution and accelerate them to contribute to the LHCD.

In this paper, a quasilinear analysis of the absorption of IBW by the electron population of the plasma is performed. It uses the analytical calculation of the amplitude of the electric field along the trajectory to obtain the quasilinear diffusion coefficient and the perturbed electron distribution function. The damping of the IBW is also calculated on the tail of the distribution function generated by the previous application of LHCD which has bridged the $n_{||}$-gap. This calculation is particularly relevant because of the IBW/LHW experiments on the Princeton Beta Experiment-Modified (PBX-M)[8] device aimed at demonstrating the synergy between IBW and LHCD.

By following N. Fisch,[9] and N. Fisch and C.F.F. Karney,[10] the Fokker-Planck equation, which shows the evolution of the distribution function, is analytically solved in only one dimension of velocity space (parallel to the magnetic field) but kept Maxwellian in the perpendicular direction. This means that only the electron

parallel dynamics has been retained in the calculation, while the ion dynamics has been assumed not to affect this process. This is because the IBW interacts only with the electron population of the plasma in the PBX-M experiment. From a mathematical point of view, this is a considerable simplification, since it allows one to obtain an analytical expression for the electron distribution function and, therefore, the damping.

In the two-dimensional case (parallel and perpendicular velocity), a numerical integration of the Fokker-Planck equation is performed together with the dynamical evolution of the IBW+LHW ray trajectories. The 2-D Fokker-Planck solver[11,12] includes the relativistic collision operator derived by B. Braams and C.F. Karney,[13] and does not use the asymptotic expansion valid for velocity three to four times greater than the thermal velocity. The numerical and analytical calculations of the distribution function are compared, and the limits of validity of the analytical theory are characterized.

The paper is organized as follows: in Sec. II, the amplitude transport equation is solved along the IBW-ray trajectory, and the parallel and perpendicular components of the electric field are calculated by using the polarization rules. In Sec. III, the quasilinear diffusion coefficient is obtained, together with the electron distribution function in the resonant region of the velocity space for both IBW and LHW. In Sec. IV, the IBW damping on the analytical electron distribution function, which is flattened by the presence of LHCD in a large interval of the parallel velocity, is calculated and the results are discussed. Sec. V contains the numerical results and a comparison with the analytical calculation. The conclusions are reported in Sec. VI.

## II. THE AMPLITUDE TRANSPORT EQUATION

The Wentzel-Kramers-Brillouin (WKB) analysis of wave propagation in the geometric optics approximation leads to a set of ordinary differential equations for the position **r**, the wave vector **k**, the time t, and the frequency $\omega$, which are formally the classical Hamilton equations for position and momentum. At a higher order of the WKB expansion, an equation for the slowly varying amplitude of the electric field can be deduced that satisfies the Poynting theorem.[14,15,16] This equation, in the electrostatic approximation, can be written as follows:

$$\frac{d|\Phi|^2}{dt} = -|\Phi|^2 \frac{d\ln(\partial H/\partial\omega)}{dt} - |\Phi|^2 \nabla\bullet\mathbf{V}_g - 2\gamma(f_e)|\Phi|^2 \qquad (1)$$

where $\Phi$ is the amplitude of the electrostatic potential, $\mathbf{V}_g = -\frac{\partial H/\partial \mathbf{k}}{\partial H/\partial\omega}$ is the group velocity of the wave packet, $\gamma$ is the wave damping rate, which in the quasilinear regime is a function of the electric field itself through the electron distribution function $f_e$ (solution of the Fokker-Planck equation), and H is the IBW electrostatic dispersion relation.

Equation (1) is nonlinear because generally, the damping term depends on the first derivative of the distribution function in velocity space calculated at the resonant velocity point $v_{||}=\omega/k_{||}$. The distribution function $f_e(t,v_{||})$, in a quasilinear theory, is obtained by solving the Fokker-Planck equation with a quasilinear diffusion term that depends on the strength of the electric field itself, as shown in Refs. 9,10. In the simple case we are considering, the one-dimensional Fokker-Planck equation can be analytically integrated to

obtain an analytical expression of $f_e(v_{||})$ for $t\rightarrow\infty$ (steady state), as will be shown below.

Equation (1) can be solved by the method of successive substitutions (Picard's method), i.e. :

$$\frac{\Phi^2_{n+1}}{\Phi_0^2} = \exp\left( - \int_0^t f(t)\,dt \; - \; 2\int_0^t \gamma(t, f_e(\Phi_n^2))\,dt \right) \qquad (2)$$

where $\Phi_0$ is the electrostatic potential at the plasma edge, the function f(t) is defined as:

$$f(t) = \frac{d\ln(\partial H/\partial\omega)}{dt} + \nabla\bullet\mathbf{V}_g \qquad (3)$$

and the damping $\gamma$ depends on the field, at the previous iteration, through the electron distribution function.

The integral of Eq. (3) that appears in Eq. (2) can be analytically solved using the solution of the ray equations given in Refs. 2,3, where the following simplified IBW dispersion relation was obtained as:

$$H = 1 - \frac{1}{2}\frac{m_i}{m_e}\left(\frac{\eta}{N\varepsilon\delta_0}\right)^2 \tau_i(x) n_{||}^2 - \frac{\delta_0}{\pi^{1/2}\eta x n_\perp(x)\tau_i^{1/2}(x)} = 0 \qquad (4)$$

In Eq. (4), $\tau_i(x)$ is the adimensional ion temperature profile, $\delta_0=\frac{c}{\omega a}$ , a is the plasma radius, $\eta=\frac{\rho_i(0)}{R_0}$ is the ratio between the ion Larmor radius and the major radius of the tokamak calculated at the plasma center, N is the ion harmonic number, $\varepsilon$ is the inverse aspect ratio, $n_\perp$ and $n_{||}$ are the perpendicular and parallel refractive indices,

respectively, and x is the normalized radial variable that measures the distance from the resonance layer, which, for the sake of simplicity, has been placed at the plasma center.

In the dispersion relation, Eq. (4), the parallel wave number depends on the radial and poloidal variables. After an integration of the ray equations,[2,3] we obtain an expression for the parallel wave number which oscillates along the trajectory as follows:

$$n_{||}(x) = \Lambda(x)\left(-C_1 \sin \nu^{1/2} I(x) + C_2 \cos \nu^{1/2} I(x)\right) \tag{5}$$

The amplitudes $C_1$ and $C_2$ are related to the plasma parameters by:

$$C_1 = \varepsilon \delta_0 \delta_T^{-1/2} \eta^{-1} \left(\frac{m_e}{m_i}\right)^{1/2} N\theta_0$$

$$C_2 = n_{||0} \tag{6}$$

$$\Lambda(x) = \left(\frac{T_i(a)}{T_i(x)}\right)^{1/4} \left(\frac{q_a}{q(x)}\right)^{1/2}$$

where $\delta_T = \frac{T_i(a)}{T_i(0)}$, $T_i(x) = T_i(0)\tau_i(x)$ with $T_i(0)$ and $T_i(a)$ being the central and edge ion temperatures, respectively, $\theta_0$ is the poloidal launching angle, and $n_{||0}$ is the value of the parallel refraction index at the antenna. The phase $I(x)$ is given by:

$$I(x) = \ln\left(\frac{x(1+x_c^2)^{1/2}}{(x^2+x_c^2)^{1/2}}\right) \tag{7}$$

with $x_c = \left(\frac{q_a}{q_0} - 1\right)^{-1/2}$, and $\nu = \left(\frac{m_i}{m_e}\right)\frac{1}{\pi N^2 q_0^2} >> 1$, which signifies a rapid oscillation of the value of $n_{||}$ near the plasma center. Equation (5) can be written concisely as:

$$n_{||}(x) = \rho(x,\theta_0,n_{||0})\cos\left(\nu^{1/2}I(x) + \arctan\frac{C_1}{C_2}\right) \qquad (8)$$

with:

$$\rho(x,\theta_0,n_{||0}) = \Lambda(x)\left(C_1^2+C_2^2\right)^{1/2} \qquad (9)$$

Figure (1) is a plot of $n_{||}$ vs. x for a bundle of rays starting at different poloidal angles $-15°<\theta_0<15°$ (for PBX-M this angle width corresponds to an 11-cm-high IBW antenna), with a uniform distribution of power along $\theta$, and $6\le n_{||0}\le 12$ for typical plasma parameters of PBX-M. These are: $n_e(0)=5X10^{13}$ cm$^{-3}$, $n_e(a)=5X10^{12}$ cm$^{-3}$ (central and edge density, respectively, with parabolic profile), $T_i(0)=T_e(0)=1.5$KeV, $T_i(a)=T_e(a)=150$eV (central and edge ion and electron temperatures, respectively, with parabolic profiles), $B_0=1.5$T (central magnetic field), f=42x10$^6$Hz (IBW frequency), N=3 (ion harmonic number at the plasma center), a=32cm (plasma radius), $R_0=164$cm (major radius), and $q_a=3$, $q_0=1$ (edge and central safety factors).

Figure (1) shows the evolution of the parallel wave number according to the predicted oscillating behavior. The $n_{||}$-width of the launched spectrum remains finite everywhere inside the plasma. This is due to the presence of the phase shift (the term $\arctan\left(\frac{C_1}{C_2}\right)$),

which depends on the poloidal injection angle. If we assume the wave damping to be very small compared to the other terms in the amplitude transport equation (Eq. (1)) ($\gamma \approx 0$), the evolution of the amplitude of the electrostatic potential for each component of the wave spectrum can be obtained by simple integration of Eq. (3) along the ray trajectory:

$$\Phi^2(x,n_{||}) = \left(\frac{T_i(a)}{T_i(x)}\right)^{1/2} \left(\frac{1+\varepsilon}{1+\varepsilon x}\right) \frac{\exp(\vartheta)}{x^2} \; \Phi_0^2(n_{||}) \tag{10}$$

where $\vartheta$ is given by:

$$\vartheta = -\frac{\varepsilon}{4}\sigma^2 \left\{\cos\left(2\arctan\frac{A_1}{A_0}\right) - x\cos\left[2\left(\nu^{1/2}\ln x + \arctan\frac{A_1}{A_0}\right)\right]\right\}$$

$$\sigma = \left(A_1^2 - A_0^2\right)^{1/2} \tag{11}$$

$$A_1 = -\left(\frac{m_i}{m_e}\right)^{1/2} \frac{\eta \delta_T^{1/2}}{N} \frac{n_{||0}}{\varepsilon \delta_0} \left(\frac{q_0}{q_a}\right)$$

$$A_0 = \theta_0$$

and $\Phi_0(n_{||})=\Phi(x=1,n_{||})$ is the Fourier component of the amplitude of the electric field at the antenna. In regions where the field diverges ($x \approx 0$), integration of the full wave equation is required to obtain the correct behavior of the field. The calculation of the quasilinear diffusion coefficient requires the knowledge of the electric field components parallel and perpendicular to the external magnetic field.

These components are evaluated performing the gradient of the electrostatic potential in the parallel and perpendicular directions:

$$E^2_{\|}(x,n_{\|})=E(x,n_{\|0})E^2_0(n_{\|})$$

$$E(x,n_{\|0}) = \frac{n^2_{\|}(x)}{n^2_{\|0}} \left(\frac{T_i(a)}{T_i(x)}\right)^{1/2} \left(\frac{1+\varepsilon}{1+\varepsilon x}\right) \frac{\exp(\vartheta)}{x^2} \qquad (12)$$

In particular, when launching waves on the equatorial plane $\theta_0=0$, the function $E(x,n_{\|0})$ reduces to:

$$E(x) = \Lambda^2(x)\, \cos^2\left(\nu^{1/2} I(x)\right) \left(\frac{T_i(a)}{T_i(x)}\right)^{1/2} \left(\frac{1+\varepsilon}{1+\varepsilon x}\right) \frac{\exp(\vartheta)}{x^2} \qquad (13)$$

and the expression for the field can be resolved into factors of two functions, one depending on the radial variable, the other on the wave spectrum. The perpendicular component of the field is:

$$E^2_{\perp}(x,n_{\|}) = \frac{n^2_{\perp}(x)}{n^2_{\|}(x)} E^2_{\|}(x,n_{\|}) \qquad (14)$$

In Eq. (12), we can choose a Gaussian wave energy density spectrum at the antenna $E^2_0(n_{\|})=C\exp\left\{-\left[(n_{\|}-n_{\|p})/\delta n_{\|}\right]^2\right\}$, where $n_{\|p}$ is the spectrum peak value, $\delta n_{\|}$ is its width, and $C=\left[(\pi)^{1/2}\delta n_{\|}\right]^{-1}$ is the normalization constant We can, then, plot (Fig. (2a,b)) the evolution of any spectral component along the parallel direction, normalized to the total field at the antenna, vs. the radial variable x for $\theta_0=0°$ (a) and $\theta_0=15°$ (b), for the plasma parameters of Fig. (1). The parallel component of the field mainly follows the behavior of the parallel refraction index. In Fig. (3a,b), the 3-D plot of Fig. (2a,b) is given vs. x and $n_{\|0}$ (the initial

wave number) for both angles $\theta_0=0°$ (a) and $\theta_0=15°$ (b). A slight amplification of the parallel component of the field occurs in relation to the peak values of $n_{||}$ (Fig. (2a)), with a greater amplification for poloidal launching angles $|\theta_0|>0°$ (Fig. (2b)).

Knowledge of the evolution of the electric field inside the plasma allows one to calculate the quasilinear diffusion coefficient everywhere in the plasma. Consequently, the distribution function for the electrons along the parallel velocity can be evaluated, assuming that $f_e$ is Maxwellian in the perpendicular direction. In the next section, we will calculate the quasilinear diffusion coefficient. Then, by simple integration of the collisional Fokker-Planck equation,[9] we will determine the evolution of $f_e$ as a function of the radial variable and the parallel velocity. The crucial parameter is the ratio between the quasilinear diffusion coefficient and the collisional diffusivity. If this parameter is high enough, there will be a considerable distortion of the distribution function from the Maxwellian. However, if the collisions are more important than the diffusion induced by the electric field, they will tend to restore the Maxwellian electron distribution function, and the effects of the field on the plasma will be negligible.

## III. THE IBW/LHW QUASILINEAR DIFFUSION COEFFICIENTS

Diffusion of the electrons in the velocity space can be induced by the presence of IBW and/or LHW parallel electric fields in the plasma for a range of values of $n_{||}$ launched by the antenna, which vary along the trajectory according to Eq. (5) in the IBW case. The quasilinear diffusion coefficient is defined[14] as:

$$D_{ql}(v_{||},x) = \pi \left(\frac{e}{m_e}\right)^2 \int_{-\infty}^{+\infty} \in (k_{||},x)\delta(\omega - k_{||}v_{||})dk_{||} \qquad (15)$$

where $\in (k_{||},x)=\frac{|E_{||}(k_{||},x)|^2}{L_\infty}$ is the wave energy density per unit interval of wave number space. Performing the integral of Eq. (15), we have:

$$D_{ql}(v_{||},x) = \left(\frac{e}{m_e}\right)^2 \frac{\pi}{v_{||}} \in \left(k_{||}=\frac{\omega}{v_{||}};x\right) \qquad (16)$$

where, for an IBW electric field, we have $\in (k_{||},x)=E(x)\in (k_{||})$ (Eqs. (12) and (13)) for equatorial wave launching.

After straightforward calculations, the average (along the $B_0$-parallel direction z) electric field energy density is given by:

$$\left\langle \frac{E^2}{8\pi} \right\rangle_z = \int_{-\infty}^{+\infty} \in (k_{||})dk_{||} \qquad (17)$$

demonstrating what we stated before, i.e., $\in (k_{||})$ is the wave energy density per unit interval of wave number space.

Substituting Eq. (12) in Eq. (16) and taking, for the sake of simplicity, a uniform wave spectrum in the interval $k_{II1}<k_{II}<k_{II2}$, the IBW quasilinear diffusion coefficient can be written as follows:

$$D^{ib}_{qI}(x,u) = \pi \left(\frac{e}{m_e}\right)^2 \left(\frac{1}{uv_{the}}\right)\left(\frac{E(x)}{\Delta k_{II}}\right) \left\langle \frac{E^2}{8\pi} \right\rangle_z \qquad (18)$$

where $u= \frac{v_{II}}{v_{the}}$ is the velocity parallel to $B_0$ and normalized to the electron thermal velocity, and $\Delta k_{II}=k_{II2}-k_{II1}$ is the width of the IBW wave spectrum, which is a function of the radial variable. The quasilinear diffusion coefficient in Eq. (18) has the dimensions of a squared velocity over time ($l^2/t^3$). It can be broken into two factors, one depending on x and the other on u. Moreover, $D_{qI}$ can be directly related to the injected wave energy at the antenna.

The quasilinear diffusion coefficient for LHW has been calculated, for simplicity, in the case of a uniform wave spectrum at the antenna, assuming a cylindrical plasma. In this case, the propagating wave energy density for an electrostatic LHW is given by:

$$E_{II}^2(x,k_{II}) = \frac{(-\varepsilon_{zz}\varepsilon_{xx})_0^{1/2}}{x(-\varepsilon_{zz}\varepsilon_{xx})^{1/2}} E_{II}^2(x=1,k_{II}) \qquad (19)$$

where:

$$\varepsilon_{xx} = 1 - \frac{\omega_{pi}^2}{\omega^2 - \Omega_{ci}^2} - \frac{\omega_{pe}^2}{\omega^2 - \Omega_{ce}^2} \approx 1$$

$$\varepsilon_{zz} = 1 - \frac{\omega_{pi}^2}{\omega^2} - \frac{\omega_{pe}^2}{\omega^2} \approx - \frac{\omega_{pe}^2(x)}{\omega^2} \qquad (20)$$

for the lower hybrid range of frequencies.

Substituting Eq. (20) in Eq. (19) and then in Eq. (16), the quasilinear diffusion coefficient for LHW is obtained:

$$D^{lh}_{ql}(x,u) = \pi \left(\frac{e}{m_e}\right)^2 \left(\frac{1}{uv_{the}}\right) \left(\frac{\left(n_e(a)/n_e(0)\right)^{1/2}}{x n^{1/2}(x)}\right) \left(\frac{1}{\Delta k_{||}}\right) \left\langle \frac{E^2}{8\pi} \right\rangle_z \qquad (21)$$

where $n(x)$ is the adimensional density profile, $n_e(a)$ and $n_e(0)$ are, respectively, the edge and the central value of the plasma density, and $\Delta k_{||}$ is the width of the launched LHW spectrum, which in the case of a cylindrical geometry does not vary along the ray trajectory. The ad-hoc assumption of the filling of the spectral gap has been made so the width of the wave spectrum extends from low values (just above the accessibility condition) to high values (three or four times the electron thermal velocity).

The diffusion due to the collisions is defined as:

$$D_{coll}(x) = \nu_0 v_{the}^2 = \frac{\omega_{pe}^4(x)\, \ln\Lambda}{4\pi n_e(x) v_{the}(x)} \qquad (22)$$

where $\nu_0$ is the electron-electron collision frequency, which decreases by increasing the electron temperature and increases by

increasing the plasma density. $n_e(x)=n_e(0)n_e(x)$ is the plasma density, $\omega_{pe}(x)$ is the electron plasma frequency, $v_{the}(x)$ is the thermal velocity, and $\ln\Lambda$ is the Coulomb logarithm, which is approximately 20 for $T_e \leq 10$ keV.

The function:

$$D_{IBW}(x) = \frac{uD^{ib}_{ql}}{D_{coll}} = \pi \left(\frac{e}{m_e}\right)^2 \left(\frac{1}{\nu_0 v_{the}^3}\right) \left(\frac{E(x)}{\Delta k_{||}}\right) \left\langle \frac{E^2}{8\pi} \right\rangle_z \qquad (23)$$

(plotted vs. the radial variable x in Fig. (4) for typical PBX-M plasma parameters with a moderate level of IBW power (0.2 KW/cm$^2$)) depends only on x. It is proportional to $\cos\left(\nu^{1/2} I(x)\right)$, and ranges from very high values, at points where the cosine is equal to one, to zero at points where the cosine is zero. For the LHW we have:

$$D_{LHW}(x) = \frac{uD^{lh}_{ql}}{D_{coll}} = \pi \left(\frac{e}{m_e}\right)^2 \left(\frac{1}{\nu_0 v_{the}^3}\right) \left(\frac{\left(n_e(a)/n_e(0)\right)^{1/2}}{x n^{1/2}(x)}\right) \left(\frac{1}{\Delta k_{||}}\right) \left\langle \frac{E^2}{8\pi} \right\rangle_z \qquad (24)$$

For an LH coupled power of about 0.5 kW/cm$^2$ and a frequency $f=4.6\text{X}10^9$ Hz, $D_{LHW}$ is much greater than unity near the plasma center.

The resonant parallel velocity $u(x)=(v_{||}/v_{the})=c/(n_{||}v_{the})$, for the case shown in Fig. (1), is proportional to $\csc\left(\nu^{1/2} I(x) + \text{arctg}\frac{C_1}{C_2}\right)$, meaning that in regions where $n_{||}(x)$ goes to zero, u(x) goes to infinity. However, in these regions, the parallel electric field approaches zero as well as the quasilinear diffusion coefficient, meaning that the electron distribution function is Maxwellian. The width of the launched spectrum in the velocity space inside the plasma is:

$$\Delta u(x) = \frac{1}{\mathrm{Min}\left(n_{||}(n_{||0},\theta_0)\right)} - \frac{1}{\mathrm{Max}\left(n_{||}(n_{||0},\theta_0)\right)} =$$

$$= \frac{\left(\mathrm{Max}\left(n_{||}(n_{||0},\theta_0)\right) - \mathrm{Min}\left(n_{||}(n_{||0},\theta_0)\right)\right)}{\mathrm{Max}\left(n_{||}(n_{||0},\theta_0)\right)\mathrm{Min}\left(n_{||}(n_{||0},\theta_0)\right)} \qquad (25)$$

In the case of equatorial launching of waves ($\theta_0$=0), the quantity $\Delta u$ of Eq. (25) reduces to:

$$\Delta u = \frac{c(n_{||02} - n_{||01})}{v_{the}\Lambda(x)n_{||02}n_{||01}} \csc\left(\nu^{1/2}I(x)\right) \qquad (26)$$

When the argument of the cosecant is zero, i.e., in regions where the parallel wavenumber goes to zero, the width $\Delta u$ becomes infinite. In these regions also the electric field goes to zero, and the distribution function reduces to a Maxwellian. In the case of $\theta_0 \neq 0$ and for a launched spectrum of $\theta_0$-values $-15° \leq \theta_0 \leq 15°$, it is necessary to solve Eq. (25) numerically. The result is given in Fig. (5), where a plot of Eq. (25) is shown vs. x for the plasma parameters of Fig. (1). The width $\Delta u$ (the distance between the dashed and the solid line in the velocity space of Fig. (5)) is finite at the plasma edge (x=1) and for $1<x<0.9$; at the point $x \approx 0.9$, $\mathrm{Min}\left(n_{||}(n_{||0},\theta_0)\right)=0$. It becomes infinite in the positive half-plane when $\mathrm{Min}\left(n_{||}(n_{||0},\theta_0)\right)$ tends to zero from the right ($x \rightarrow 0.9$), and infinite in the negative half-plane when it tends to zero from the left. It is still finite in the negative half-plane for $0.55<x<0.6$ and infinite when $x \rightarrow 0.55$ and $x \rightarrow 0.6$ at points where $\mathrm{Max}[n_{||}(n_{||0},\theta_0)]$ goes to zero. The vertical asymptotes, in the plane (u-x), indicate the points where $n_{||}(n_{||0},\theta_0)=0$. Nonetheless, due to the variation of $n_{||}$ along x, the wave spans the whole of velocity space. This means that during

its propagation, the wave is able to distort the distribution function at all velocities. However, it is clear that when $n_{||} \rightarrow 0$ ($u \rightarrow \infty$) the parallel electric field goes to zero (i.e., Eq. (12)). Here the quasilinear diffusion coefficient will be too small to distort the distribution function. It is reasonable to suggest that the IBW can affect the behavior of the distribution function only for low parallel velocities on both sides (i.e., positive and negative values of u).

The solution of the 1-D Fokker-Planck equation, when IBW and LHW are concurrently present, is given by the Fisch formula[9]

$$f_e(u,x) = C_0 \exp\left( - \int^{u} \frac{udu}{1 + u^3 \left( \frac{D^{ib}_{ql}(x,u) + D^{lh}_{ql}(x,u)}{D_{coll}} \right)} \right) \qquad (27)$$

Substituting Eqs. (18), (21) and (22) in Eq. (27), and using the functions $D_{IBW}(x)$ and $D_{LHW}(x)$, which are independent of u, the integral of Eq. (27) can be analytically evaluated to obtain:

$$f_e(u,x) = C_0 \left( \frac{1}{\left( D_{IBW}(x) + D_{LHW}(x) \right)} + u^2 \right)^{-\alpha} \qquad (28)$$

where:

$$\alpha = \frac{1}{2\left( D_{LHW}(x) + D_{IBW}(x) \right)} \qquad (29)$$

for $u_1(x) = \frac{\omega}{k_{||2}(x) v_{the}} < u(x) < u_2(x) = \frac{\omega}{k_{||1}(x) v_{the}}$ (i.e., inside the wave number spectrum interval where the wave is present). Outside this

interval, the distribution function is Maxwellian. This can be verified by performing the integral in Eq. (27) for $D_{IBW}=D_{LHW}=0$.

In Eqs. (28) and (29), $D_{IBW}(x)$ and $D_{LHW}$ are given by Eqs. (23) and (24). The constant $C_0$ can be determined by the normalization of $f_e(u)$ in all of velocity space.

The effect of IBW and LHW fields on the distribution function can be seen in Eq. (28). For every radial location x, the distribution function will be distorted with respect to the Maxwellian distribution for $u_1 = \frac{\omega}{k_{II2}v_{the}} < u < u_2 = \frac{\omega}{k_{II1}v_{the}}$, i.e., inside the range of the wave spectrum interval. When $D_{LHW}(x)$ or $D_{IBW}(x)$ are sufficiently large, a significant distortion of the distribution function from the Maxwellian will take place.

In Fig. (6), a 3-D plot of the distribution function vs. u (normalized velocity) and x (radial variable) is shown for a case where only an IBW of moderate power density (0.2 kW/cm$^2$) is present in the plasma (in this case ($D_{LHW}=0$)). Fig. (7) shows a projection of the distribution function on the plane ($f_e$-$v_{II}$) for all the x-values. A large distortion of the distribution function can be noted in relation to the maxima of the parallel electric field, for typical parameters of a PBX-M circular-shaped plasma (as in Fig (1)). This can be more clearly seen in Fig. (8), where the contour plot of $f_e$ is shown with the evolution of $n_{II}$ (dashed curve).

It can be verified from Fig. (7) that IBW affects the electron distribution function on both sides of the velocity space, and in a range of values that are one to three times the thermal velocity. This behavior can be explained by the fact that the parallel wave number changes from 0 to very high values during the propagation. Moreover, the parallel electric field contributes to a significant distortion of

the distribution function only for high values of the parallel refractive index (low velocity).

It can be easily deduced that IBW alone cannot produce a net current in the plasma, unlike LHW. LHW can produce an asymmetric distortion of the distribution function in a wide range of resonant parallel velocities, generating a tail in the distribution function that extends up to large values of velocity.

In the next section, we will examine the possibility of improving the efficiency of LHCD by simultaneously launching an IBW. This is done by calculating the damping of the IBW on the tail of the distribution function generated by LHCD.

## IV. DAMPING OF THE IBW IN THE PRESENCE OF A LHW-TAIL

This section contains the calculation of the IBW damping on the distribution function tail generated by a high-power LHW. This is a typical experimental situation of PBX-M[5] where approximately 400 kW of lower hybrid wave power is coupled to the plasma in the current drive regime. After this, a shorter IBW pulse at lower power (around 100 kW) is coupled to the plasma for $6<n_{||0}<12$, and simultaneously with LHCD. The question is whether or not the power launched by the IBW could be absorbed by the electrons present in the tail generated by LHW, whose spectrum inside the plasma extends from $n_{||0}=1.8$ to 8 (filling the $n_{||}$-gap).

From Eq. (2) and the analytical solution of the integral along the trajectory of the expression in Eq. (3), we can write the formal solution for the electrostatic potential:

$$\frac{\Phi^2_{n+1}}{\Phi_0{}^2} = \left(\frac{T_i(a)}{T_i(x)}\right)^{1/2} \left(\frac{1+\varepsilon}{1+\varepsilon x}\right) \frac{\exp(\vartheta)}{x^2} \exp\left( - 2 \int_0^t \gamma(t, f_e(\Phi_n{}^2))\, dt \right) \qquad (30)$$

The damping decrement of an IBW along the ray trajectory for each Fourier component of the wave spectrum is given by:

$$\Gamma(t) = \left( - 2 \int_0^t \gamma(t, f_e(\Phi_n{}^2))\, dt \right) \qquad (31)$$

It should be noted that when two wave spectra (LHW+IBW) are simultaneously present inside the plasma, the electron distribution

function in Eq. (31) depends on both wave fields through the LHW and IBW quasilinear diffusion coefficients.

Using the ray equation $dx/dt=-\delta_0\partial_{n_x}H/\partial_\omega H$, where $n_x$ is the wave number in the radial direction, we can write $\Gamma$ as a function of x:

$$\Gamma(x) = -\frac{2}{\delta_0}\int_1^x \frac{\gamma(x,f_e(\Phi^2))}{v_{gx}}\,dx \tag{32}$$

where:

$$\gamma(x) = \frac{\mathbf{k}\bullet\underline{\varepsilon}^A\bullet\mathbf{k}}{\partial H/\partial\omega} = \frac{H^{Im}}{\partial H/\partial\omega} \tag{33}$$

$$H^{Im} = -\pi\frac{\omega_{pe}^2(x)}{v_{the}^2(x)}\left(\frac{df_e(x,u)}{du}\right)_{u=c/n_{||}v_{the}} \tag{34}$$

and:

$$v_{gx} = -\frac{\partial H/\partial n_x}{\partial H/\partial\omega} = -2\pi^{1/2}\eta\delta_0^{-1}\frac{\omega_{pi}^2(x)}{v_{thi}^2(x)}\frac{T_i^{1/2}(x)x}{\partial H/\partial\omega} \tag{35}$$

H is the IBW dispersion relation (Eq. (4)), $H^{Im}$ is the imaginary part of the dispersion relation, $v_{gx}$ is the group velocity along the radial direction, and $f_e(x,u)$, the distribution function of the electrons in the parallel direction, is given in Eq. (28).

Using Eqs. (33)-(35) in Eq. (32), we obtain:

$$\Gamma(x) = \frac{\pi^{1/2}}{\eta} \frac{T_i(0)}{T_e(0)} \int_x^1 dx \; \frac{T_i^{1/2}(x)}{T_e(x)} \left( \frac{df_e(x,u)}{du} \right)_{u=c/n_{||}v_{the}} \tag{36}$$

The integrand of Eq. (36) contains the derivative of the distribution function in the resonant velocity point $u=\omega/(k_{||}v_{the})=c/(n_{||}v_{the})$, where $n_{||}$ is the IBW parallel wave number which depends on x (Eq. (8)). The derivative of the distribution function can be calculated starting from Eq. (28). We obtain:

$$\left( \frac{df_e(x,u)}{du} \right)_{u=c/n_{||}v_{the}} = -\frac{2\alpha C_0 c}{n_{||}v_{the}} \left( \frac{1}{\left( D_{IBW}(x) + D_{LHW}(x) \right)} + \left( \frac{c}{n_{||}v_{the}} \right)^2 \right)^{-\alpha-1} \tag{37}$$

where the constant $C_0$ is determined by imposing the boundary condition on the distribution function, which, outside the interval of resonant velocity, is the usual Maxwellian function.

Equation (30) is solved by numerical iteration and the IBW energy decrement $\exp(\Gamma(x))$ is obtained for each component of the spectrum when a LHW distorts the Maxwellian profile of the distribution function ($D_{LHW} \neq 0$).

A plot of the IBW power decrement vs. x is given in Fig. (9) for typical plasma parameters of the PBX-M machine, and for only one component of the spectrum $n_{||p}=6$ when a LHW flattens the distribution function over a wide range of parallel velocities (solid curve). Clearly, this calculation must be repeated for all the parallel wavenumbers of the power spectrum, each of them carrying a fraction of the total power. On the same plot, we also show the power decrement obtained when we can neglect the effect of $D_{LHW}$ and $D_{IBW}$ (dashed curve). In this case, the distribution function is Maxwellian,

and we are considering linear damping. As shown in the figure, the quasilinear absorption is greater than the linear absorption in the space interval where the velocity space value $\left(v_{||}=\left(\frac{c}{n_{||}}\right)\right)$, corresponding to the launched IBW $n_{||}$, is more than three times the thermal velocity. This is clear from Fig. (10), where we show a plot of the distribution function along the parallel velocity for a Maxwellian case (solid curve) and a case where $D_{LHW}\neq 0$ in a central region of the plasma (dashed curve)). The slope of the tail $\left(\left(\frac{dfe}{du}\right)_{u=c/n_{||}v_{the}}\right)$ for $v_{||}/v_{the}\geq 3$, in the distorted case, is greater than in the Maxwellian case, and the power decrement is proportional to the value of the slope of the distribution function (Eq. (35)). In intervals where the IBW-$n_{||}$ value is such that the related value in the velocity space is less than $3v_{the}$, the absorption of the wave is less than in the linear case. In fact, the value of the slope of the distribution function is greater for the Maxwellian case (Fig. (10)). Thus, each component of the launched IBW can be absorbed by the plasma in zones where the wave spectrum satisfies the above conditions.

To show this point more clearly, we have plotted in Fig. (11) the interaction zones, in velocity space, between IBW and LHW as it results from the ray tracing evolution of the parallel wavenumbers. The velocity $u(x)=c/(n_{||}(x)v_{the}(x))$ (included between -10 to 10) is plotted vs. $x=r/a$ (normalized radial variable) in three cases $n_{||}(x)=n_{||IBW}(x)$ (dashed line), $n_{||LHW1}(x)$ (triangles), $n_{||LHW2}(x)$ (circles). For the LHW case, the subscripts 1 and 2 refer to the low and high boundary of the LHW spectrum, while in the IBW case we have taken the peak value of the spectrum, $n_{||p}\approx 6$. The LHW affects and modifies the distribution function in the zone included between the curves of

circles and triangles. When LHW and IBW travel in the same spatial regions, the IBW can fall in these zones in velocity space and lead to quasilinear absorption. Outside these regions, the distribution function is Maxwellian and the IBW-absorption is linear.

This analysis is based on the analytical integration of the IBW ray tracing equations with a 1-D Fokker-Planck equation using an asymptotic evaluation of the collision operator at the high velocity limit. It shows that the IBW can be absorbed by the electrons in the tail generated by the previous application of LHCD. The electrons, under the effect of the IBW electric field, would undergo a further acceleration with an increase oin the lower hybrid current drive efficiency.

The approximations used in the analytical derivation of the ray tracing equations appear to be well-tested, and the results are very accurate. However, with the analytical integration of the 1-D Fokker-Planck equation in the high velocity limit, there are some problems when the waves (IBW and LHW) interact with the low velocity plasma electrons. In this case, in fact, the asymptotic expansion is no longer valid. The next section contains the results of a numerical calculation for the dynamical evolution and damping of the interacting waves obtained using a 2-D relativistic Fokker-Planck code.

## V. NUMERICAL ANALYSIS OF THE IBW/LHW SYNERGY.

A numerical code which includes IBW and LHW ray evolution, calculation of electric fields, and quasilinear diffusion coefficients for IBW and LHW, has been coupled to a new version of a 2-D relativistic Fokker-Planck equation solver which includes the accurate Braams-Karney collision operator[11,12]. The power decrement of a 2-D propagating IBW in a non-Maxwellian background, strongly distorted by a LHW in the current drive regime, has been compared to the one obtained in the previous section using the analytical approach.

The plasma is divided into 100 layers, each characterized by a value of the poloidal flux function $\psi$, which in a polar system of coordinates corresponds to the simple equation r=const. An IBW and a LHW are launched from the plasma boundary with an imposed power spectrum. The LHW spectrum is included between a minimum and maximum value of the parallel wavenumber. On each layer the waves are characterized by the parallel wavenumber, the electric field, and the quasilinear diffusion coefficients obtained by integration of the ray-equations (WKB approximation), as described in the previous sections. At this point, the 2-D Fokker-Planck code is run assuming the wave conditions found on each layer. The 2-D distribution function and its derivative along the parallel velocity (given by the code in spherical coordinates as: $f(v,\mu)$ with $v=(v_\perp{}^2+v_{||}{}^2)$ and $\mu=\cos\phi=\cos\{\arctan\frac{v_\perp}{v_{||}}\}$) is transformed into parallel and perpendicular coordinates. The derivative along $v_{||}$ is calculated at the resonant point $v_{||}=\frac{\omega}{k_{||}v_{the}}$, and numerically integrated along $v_\perp$. The damping rate $\gamma$ can be calculated at any radial position, and finally, the power

decrement $\Gamma$ (Eq. (32)) is obtained by integration along the radial variable.

The Fokker-Planck code has been tested by running the code at every radial position in the case of zero diffusion coefficients ($D_{IBW}(x) + D_{LHW}(x)=0$). In this case, the resulting distribution function must be a Maxwellian because there are no waves interacting with the plasma electrons. The power decrement has been calculated, as described above, and compared to the analytical calculation. The result is shown in Fig. (12), where the transmitted power normalized to the coupled power has been plotted vs. x in the analytical case (circles) and numerical case (triangles). The agreement is very good.

Figure (13) shows the transmitted power (Maxwellian: dashed line and modified: solid line) vs. x for a case where an IBW is propagating in a LHW-modified background distribution function. This is the same case as in Fig. (9) of the previous section, where the result was analytically obtained. A comparison between Fig. (9) and Fig. (13) shows a very good agreement between the analytical and numerical approaches. This could be explained by the fact that, in this case, most of the power is lost for $x>0.2$, where the IBW interacts with the plasma electrons in a range of velocities such as $v_{||}>2.5v_{the}$ (see Fig. (11)).

In Fig. (14), we have plotted the transmitted power vs. the initial IBW-parallel wavenumber for a large range of values ($2\leq n_{||ibw}\leq 12$) of the spectrum at four radial positions x=0.9, 0.6, 0.3, 0.1. We compare the case of Maxwellian distribution functions (lines) with the case with LHCD in the central region of the plasma (x=0.9: circles, x=0.6: squares, x=0.3: diamonds, x=0.1: triangles). A large difference in the transmitted power is observed for x=0.1 (near the

plasma center) in the range $2 \leq n_{\parallel ibw} \leq 5$. The LHW, interacting with the electrons, modifies the distribution function and changes the absorption properties of the plasma, helping the IBW to be absorbed.

Therefore, the analytical approach provides a good description of the IBW/LHW synergy in this range of plasma parameters. We are then able to conclude that IBW can be used in conjunction with LHW to improve the current drive efficiency.

## VI. CONCLUSIONS

A quasilinear analysis of the absorption of IBW by the electron species has been analytically and numerically developed. The parallel electric field, the diffusion coefficient, and the distortion of the distribution function, caused by the presence in the plasma of a strong electric field due to IBW, have been analytically determined. This method was applied to analyze the combined effects of LHW and IBW in a typical experimental situation for the PBX-M tokamak. Numerical results for the IBW power damping rate have been obtained using a 2-D Fokker Planck code. Cross-comparisons between analytical and numerical calculations have been shown good agreement between the two approaches.

## ACKNOWLEDGMENTS

The authors would like to thank Dr. M. Shoucri who provided the 2-D Fokker-Planck routine which made possible the comparison between numerical and analytical calculations. Special appreciation is due to Dr. C. Castaldo for his useful comments on this work.

This work has been supported by the U.S. Department of Energy grants: Princeton Plasma Physics Laboratory, No. DE-AC02-76-CHO-3073; Massachusetts Institute of Technology, No. DE-FG02-91E54109.

## REFERENCES

[1] M. Ono, Phys. Fluids B **5**, 241 (1993).

[2] A. Cardinali, F. Romanelli, Phys. Fluids B **4**, 504 (1992).

[3] A. Cardinali, Phys. Fluids B **5**, 2778 (1993).

[4] A. Cardinali, S. Bernabei, D. Ignat, D. Lee, M. Ono, F. Paoletti, E. Valeo, and PBX-M group, Bull. Am. Phys. Soc. **38**, 2094 (1993).

[5] W. Tighe, R. Bell, S. Bernabei, A. Cardinali, T.K. Chu, S. Jones, R. Kaita, B. Leblanc, M. Ono, F. Paoletti, G. Petravich, H. Takahashi, S. Von Goeler, A. Post Zwicker, and PBX-M group, Bull. Am. Phys. Soc. **38**, 2094 (1993).

[6] A. Ram, A. Bers and V. Fuchs, Proceedings of the 20$^{th}$ EPS Conference on Controlled Fusion and Plasma Physics, edited by J.A. Costa, M.E. Manso, F.M. Serra, F.C. Schueller (EPS, Lisboa, Portugal, 1993), Vol. 17C part III, p. 897.

[7] C. Gormezano, Proceedings of the 10$^{th}$ Topical Conference on Radio Frequency Power in Plasmas, edited by M. Porkolab and J. Hosea, (AIP, Boston, Massachusetts, 1993), p. 87.

[8] R. Bell, N. Asakura, S. Bernabei, M.S. Chance, P.A. Duperrex, R.J. Fonck, G.M. Gammel, G.J. Greene, R.E. Hatcher, A. Holland, S.C. Jardin, T.W. Jiang, R. Kaita, S.M. Kaye, C.E. Kessel, H.W. Kugel, B. Leblanc, F.M.

Levinton, M. Okabayashi, M. Ono, S.F. Paul, E.T. Powell, Y. Qin, D.W. Roberts, N.R. Sauthoff, S. Sesnic, and H. Takahashi, Phys. Fluids B **2**, 1271 (1990).

[9] N. Fisch, Phys. Rev. Lett. **41**, 873 (1978).

[10] C.F.F. Karney and N. Fisch, Phys. Fluids **22**, 1817 (1979).

[11] M. Shoucri and I. Shkarofsky, Comput. Phys. Commun. **78**, 199 (1993).

[12] M. Shoucri and I. Shkarofsky, Comput. Phys. Commun. **82**, 287 (1994).

[13] B. Braams and C.F.F. Karney, Phys. of Fluids B **1**, 1355 (1989).

[14] T.H. Stix, Waves in Plasmas, (American Institute of Physics, New York, 1992).

[15] M. Brambilla, A. Cardinali, Plasma Phys. **22**, 1817 (1982).

[16] I. Bernstein and L. Friedland, in Plasma Physics Handbook, edited by A.A. Galeev and R.N. Sudan (North Holland, Amsterdam, 1984), Vol. 1, p. 367.

## FIGURE CAPTIONS

Fig. (1) Parallel wave number for a bundle of rays starting at-$15°<\theta_0<15°$, with $6\leq n_{\|0}\leq 12$ vs. the normalized plasma radius x for the PBX-M tokamak plasma parameters: $n_e(0)=5X10^{13}$ $cm^{-3}$, $n_e(a)=5X10^{12}$ $cm^{-3}$, $T_i(0)=T_e(0)=1.5KeV$, $T_i(a)=T_e(a)=150eV$, with parabolic profile, $B_0=1.5T$, $f=42x10^6Hz$, N=3 ($3^{nd}$ harmonic at the plasma center), $a=32cm$, $R_0=164cm$, $q_a=3$, $q_0=1$.

Fig. (2a,b) The squared amplitude of the parallel electric field normalized to the total field at the antenna vs. x for the plasma parameters of Fig. (1) and a Gaussian power spectrum at the plasma edge centered on $n_{\|p}=9$, for launching angles $\theta_0=0°$(a) and $\theta_0=15°$(b).

Fig. (3a,b) Three-dimensional plot of the parallel electric field vs. x and $n_{\|0}$ for $\theta_0=0°$(a) and $\theta_0=15°$(b) for a Gaussian power spectrum, and with the parameters of Fig. (2a,b).

Fig. (4) Quasilinear diffusion coefficient over collisional diffusivity vs. x for the parallel electric field of Fig. (2a).

Fig. (5) Maximum (dashed line) and minimum (solid line) values of the parallel velocity normalized to the thermal velocity vs. x for the spectrum of Fig. (1).

Fig. (6) Three-dimensional plot of the electron distribution function $f_e$ vs. x and u for an IBW of moderate power 0.2 $kW/cm^2$ for $D_{IBW}(x)$ of Fig. (4).

Fig. (7) The plot of Fig. (6) projected in the plane ($f_e$,u) for all x.

Fig. (8) Contour plot of $f_e(x,u)$ together with the evolution of $n_{||}(x)$ (dashed curve) for $n_{||0}=6$ and $n_{||0}=12$.

Fig. (9) Absorbed IBW power $\exp(\Gamma)$ vs. x for a Maxwellian distribution function (linear damping) (dashed line) and a modified distribution function ($D_{LHW}\approx 0.5$) (solid line), when considering only one component of the wave spectrum $n_{||p}=6$ (the peak value). The plasma parameters are the same as Fig. (1).

Fig. (10) Distribution function $f_e$ vs. u for the Maxwellian (solid line) and modified ($D_{LHW}\neq 0$) (dashed line) cases near the plasma center.

Fig. (11) Velocity $u=c/(n_{||}(x)v_{the}(x))$ vs. x for the propagating IBW (solid line) and the boundary values of the LHW spectrum (circles and triangles), with the same plasma parameters as in Fig. (1).

Fig. (12) Transmitted power vs. x in the case of a Maxwellian plasma ($D_{IBW}=D_{LHW}=0$), obtained analytically (circles) and numerically (triangles) for the same plasma parameters as in Fig. (9).

Fig. (13) Transmitted power of an IBW vs. x in the case of a Maxwellian distribution function (dashed line) and when a LHW interacts with the plasma ($D_{LHW}\neq 0$) (solid line), numerically obtained by running the 2-D Fokker-Planck code for the same plasma parameters as in Fig. (9).

Fig. (14) Transmitted power of an IBW vs. $n_{||ibw}$ for four radial positions x=0.9, 0.6, 0.3, 0.1, in the case of a Maxwellian distribution function (lines) and when a LHW interacts with the plasma ($D_{LHW}\neq 0$) (x=0.9: circles, x=0.6: squares, x=0.3: rhomboids, x=0.1: triangles), numerically obtained by running the 2-D Fokker-Planck code for the same plasma parameters as in Fig. (9).

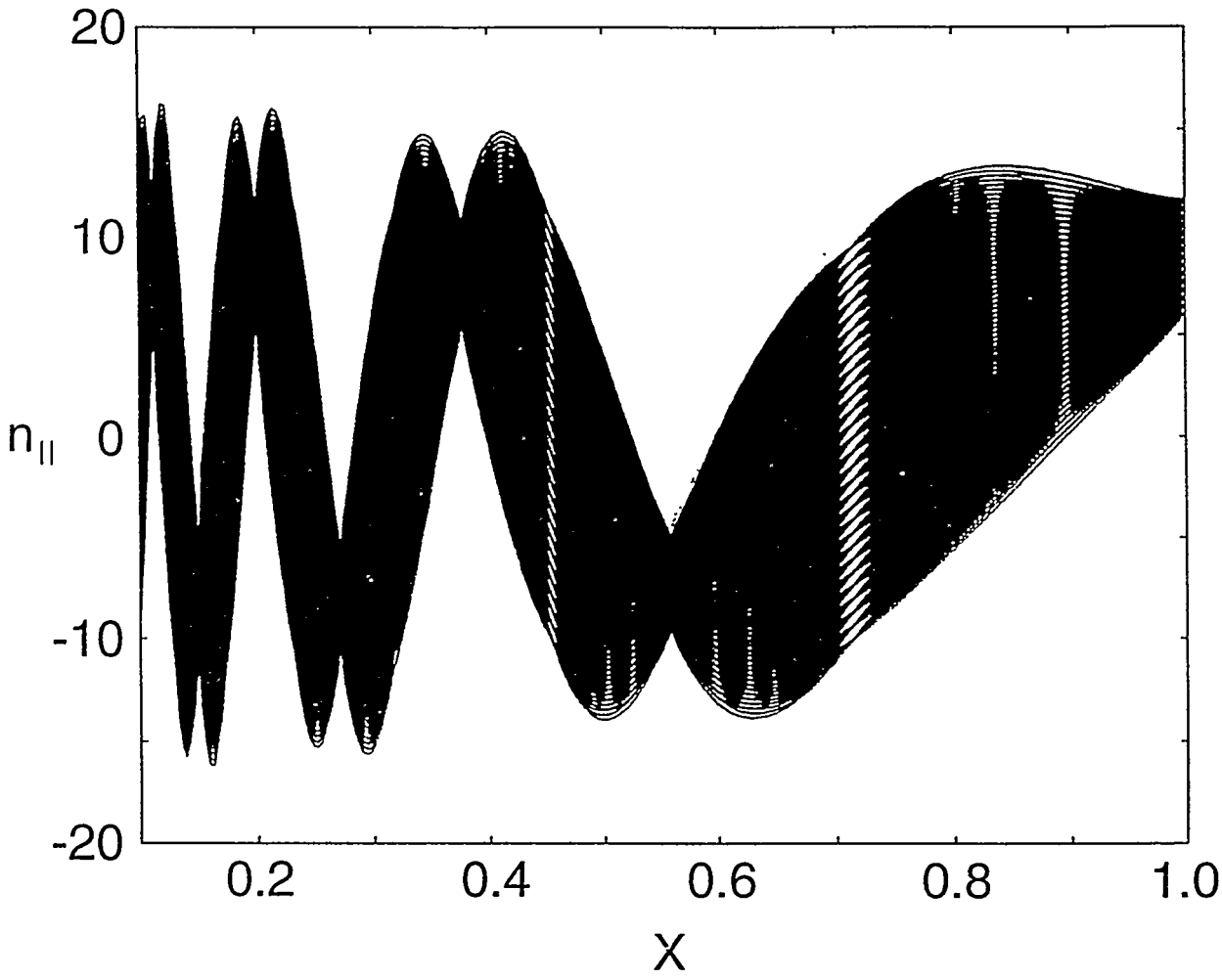


Fig. 1

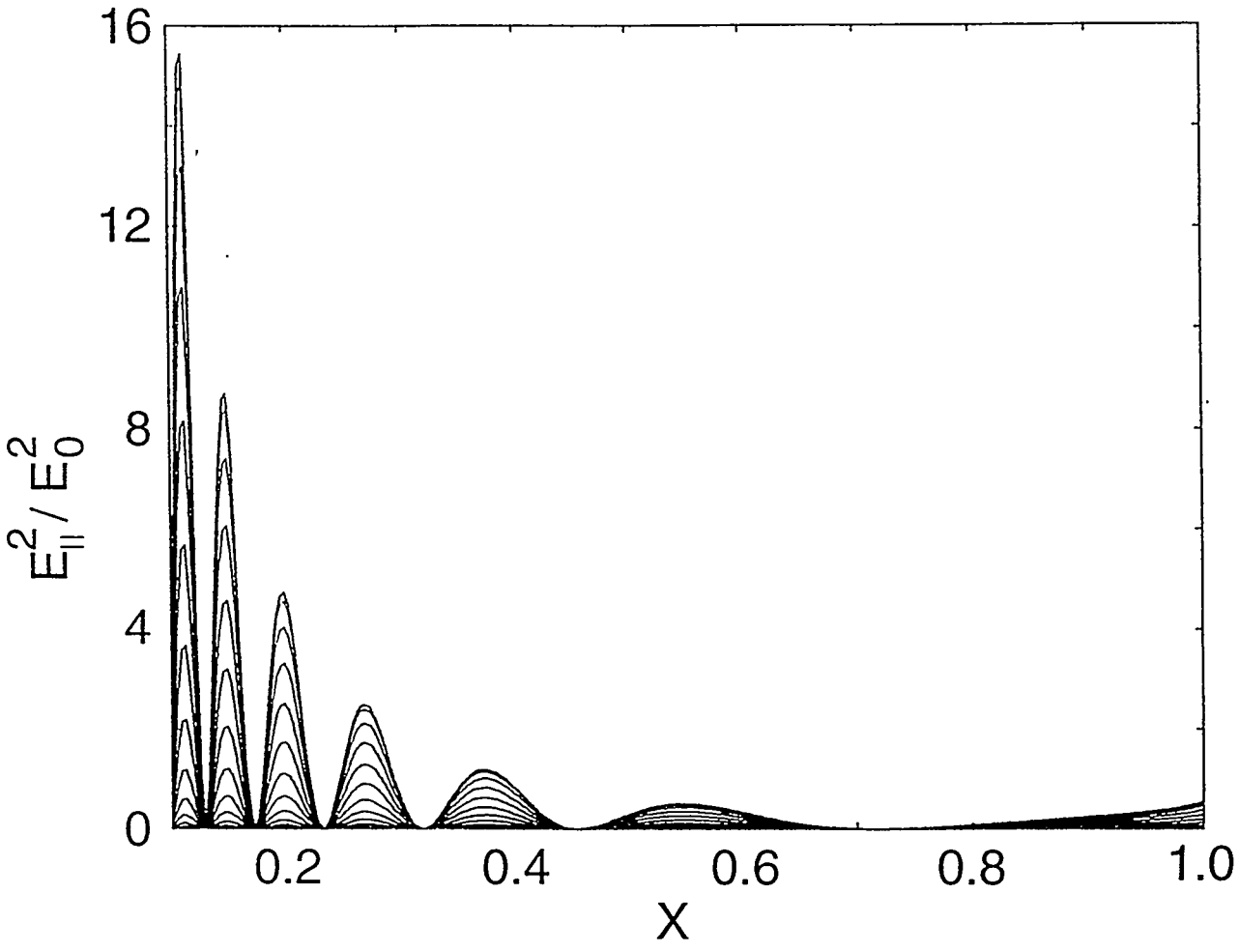


Fig. 2 (a)

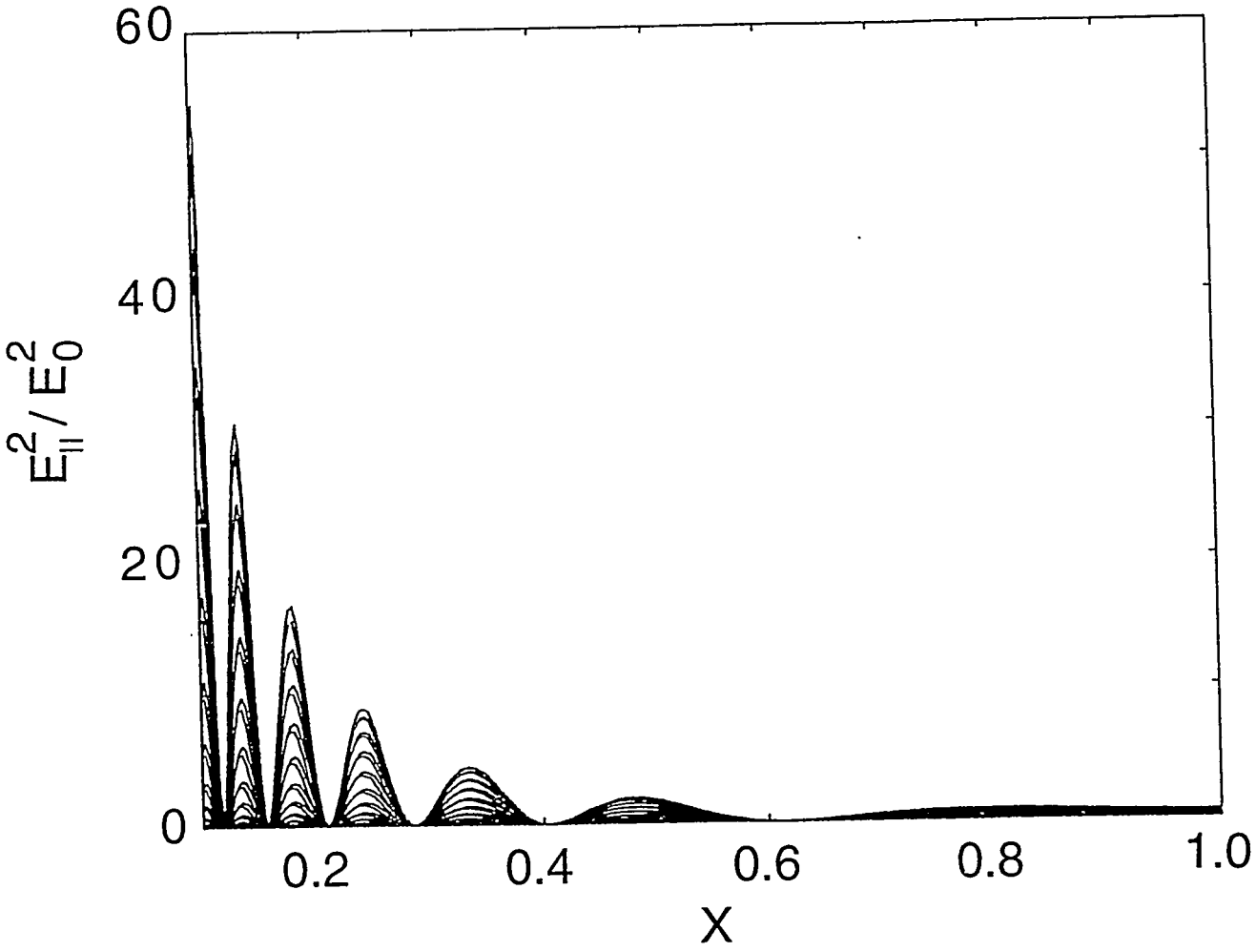


Fig. 2 (b)

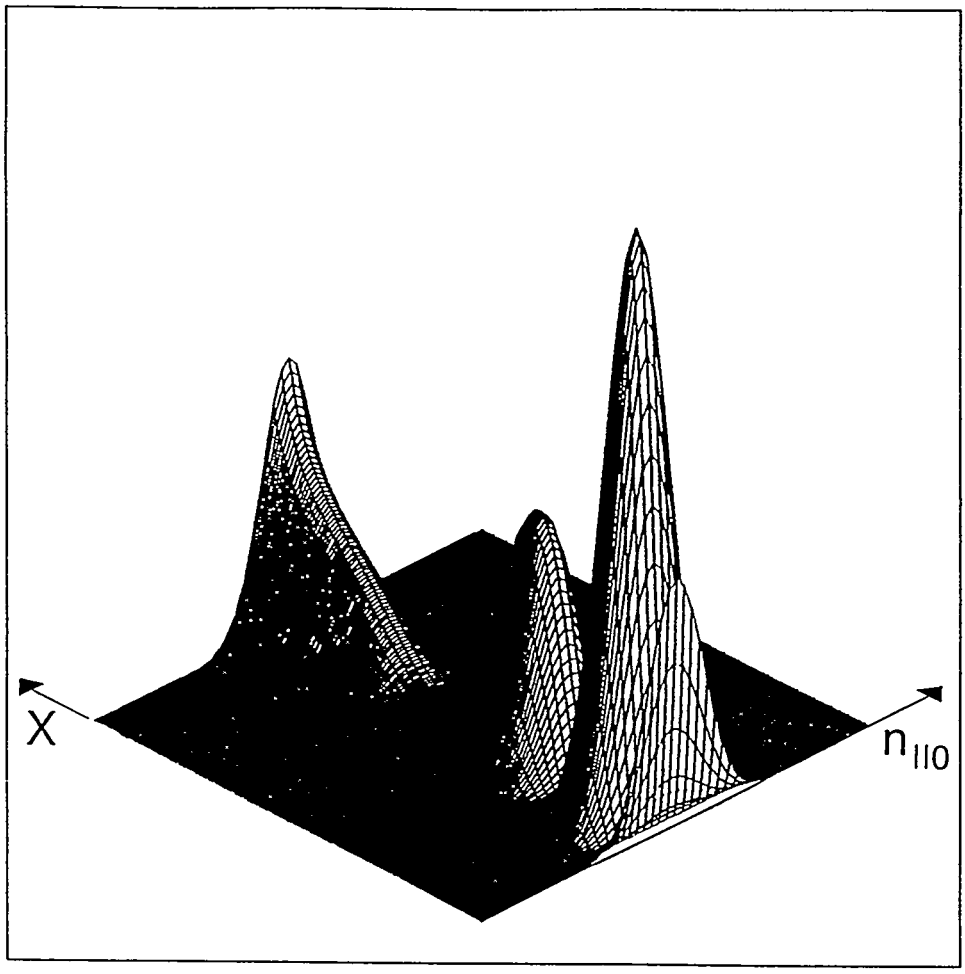


Fig. 3 (a)

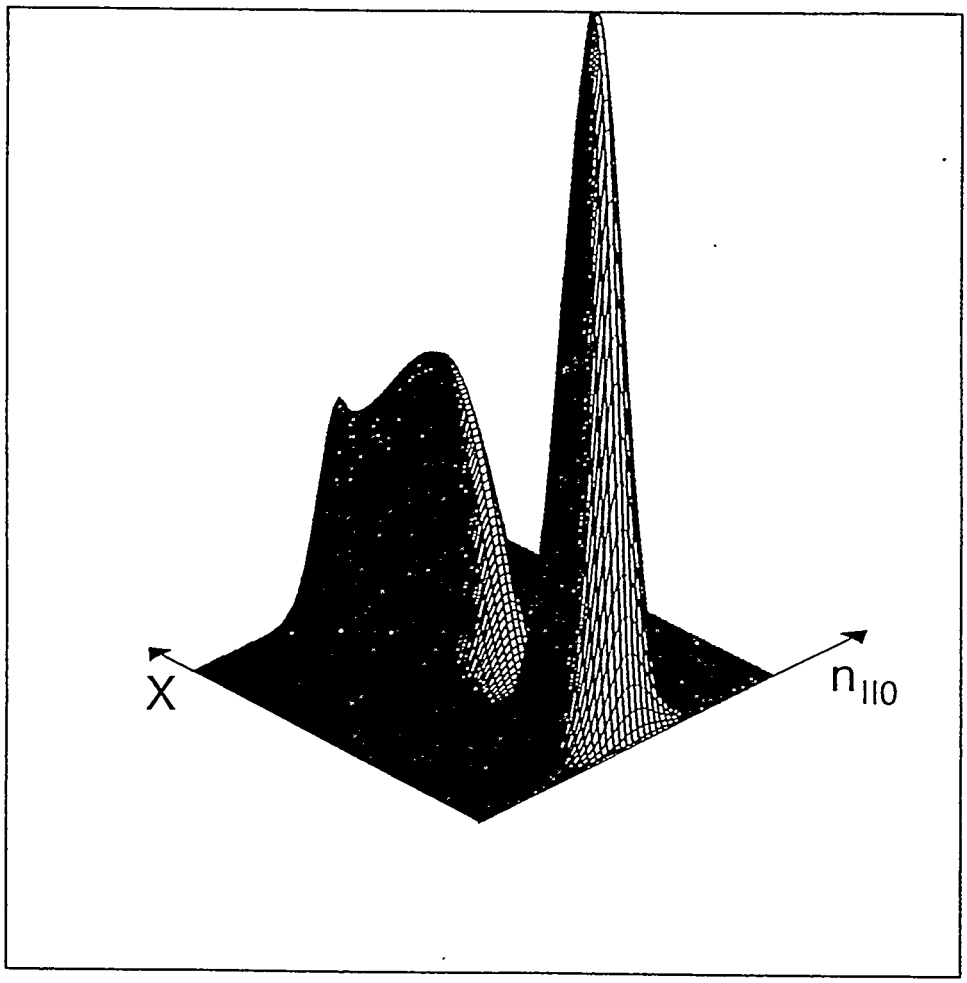


Fig. 3(b)

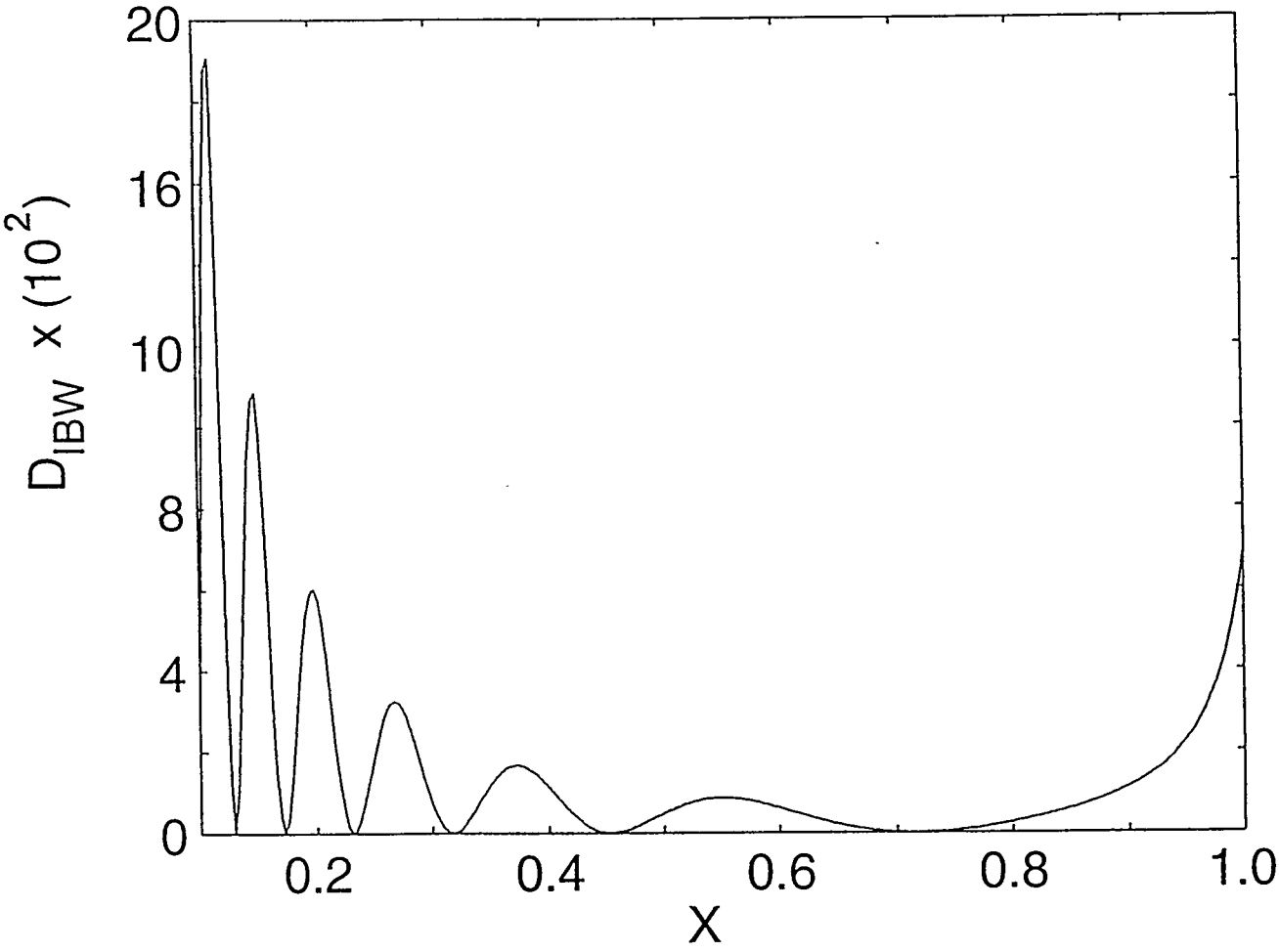


Fig. 4

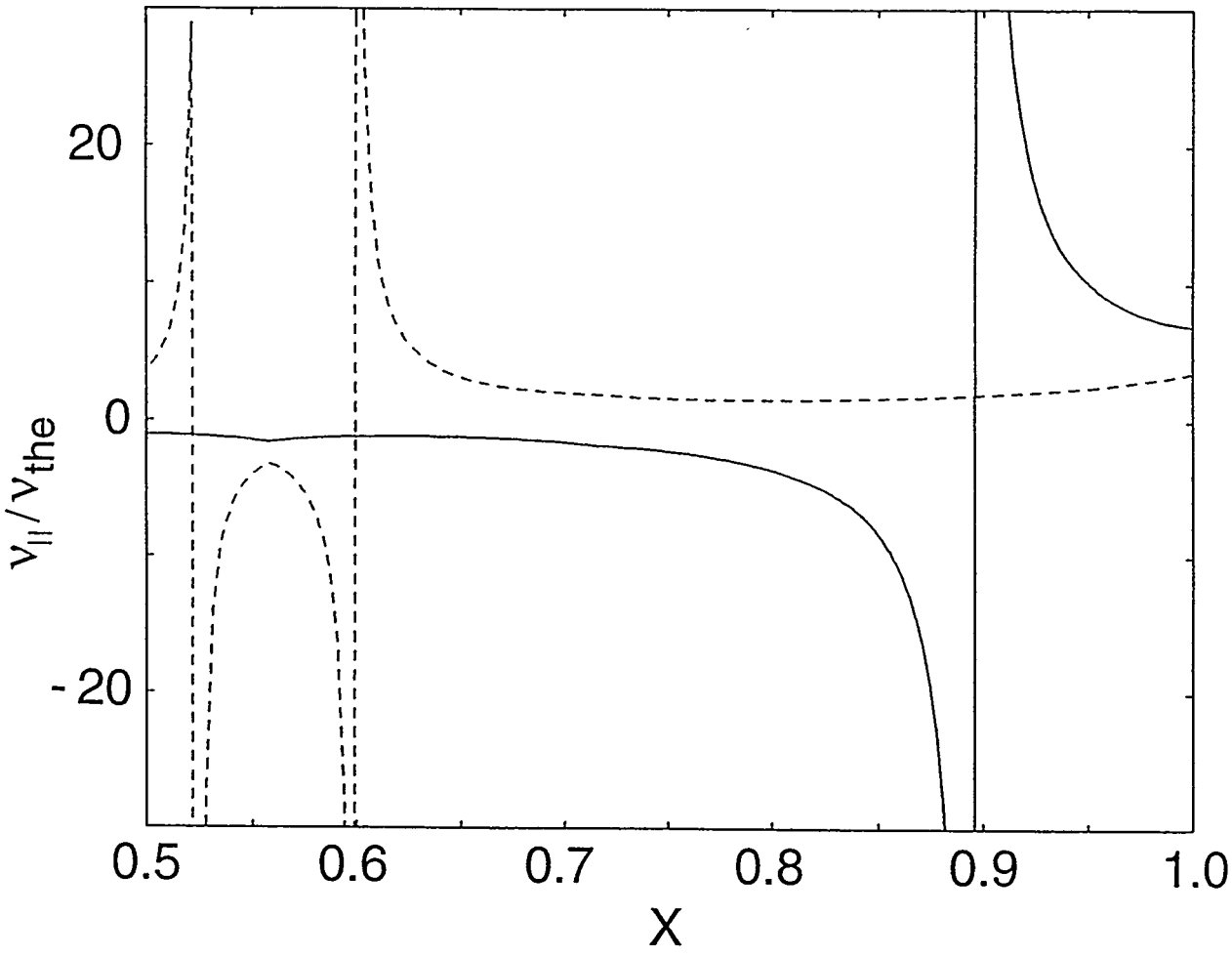


Fig. 5

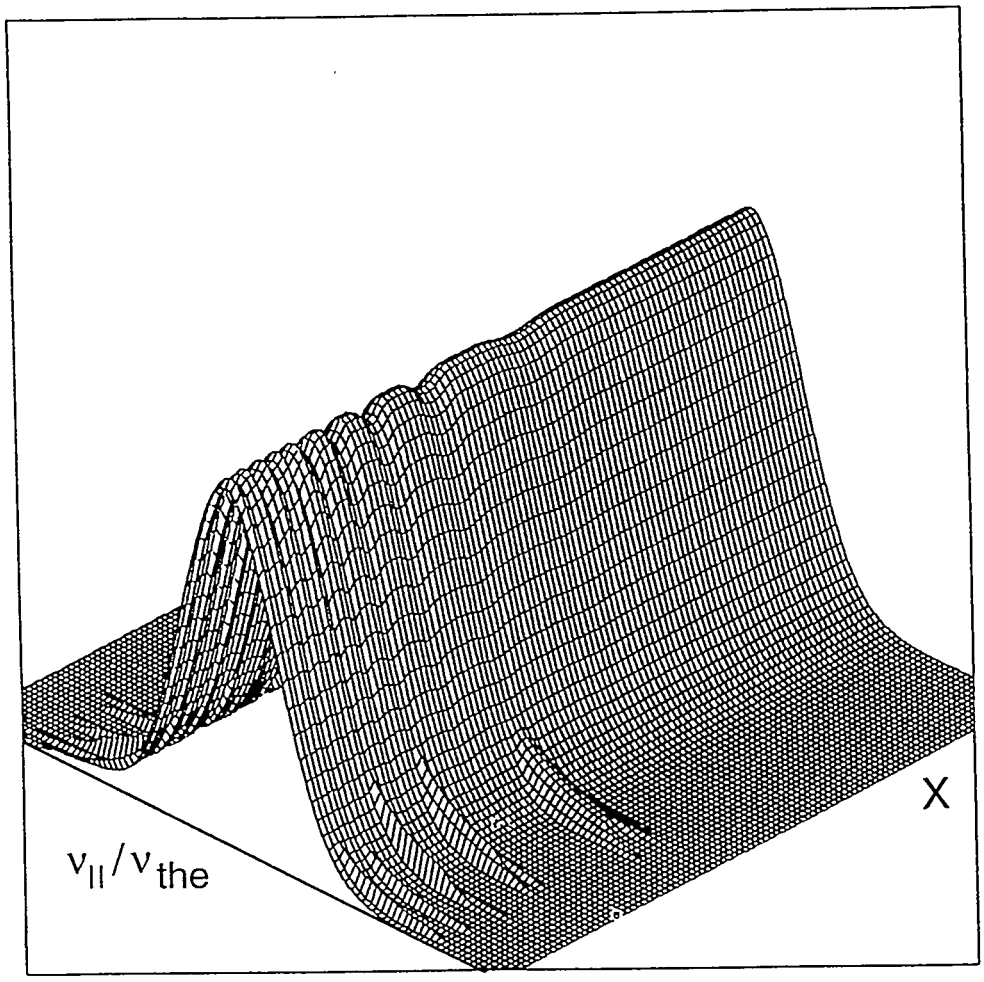


Fig. 6

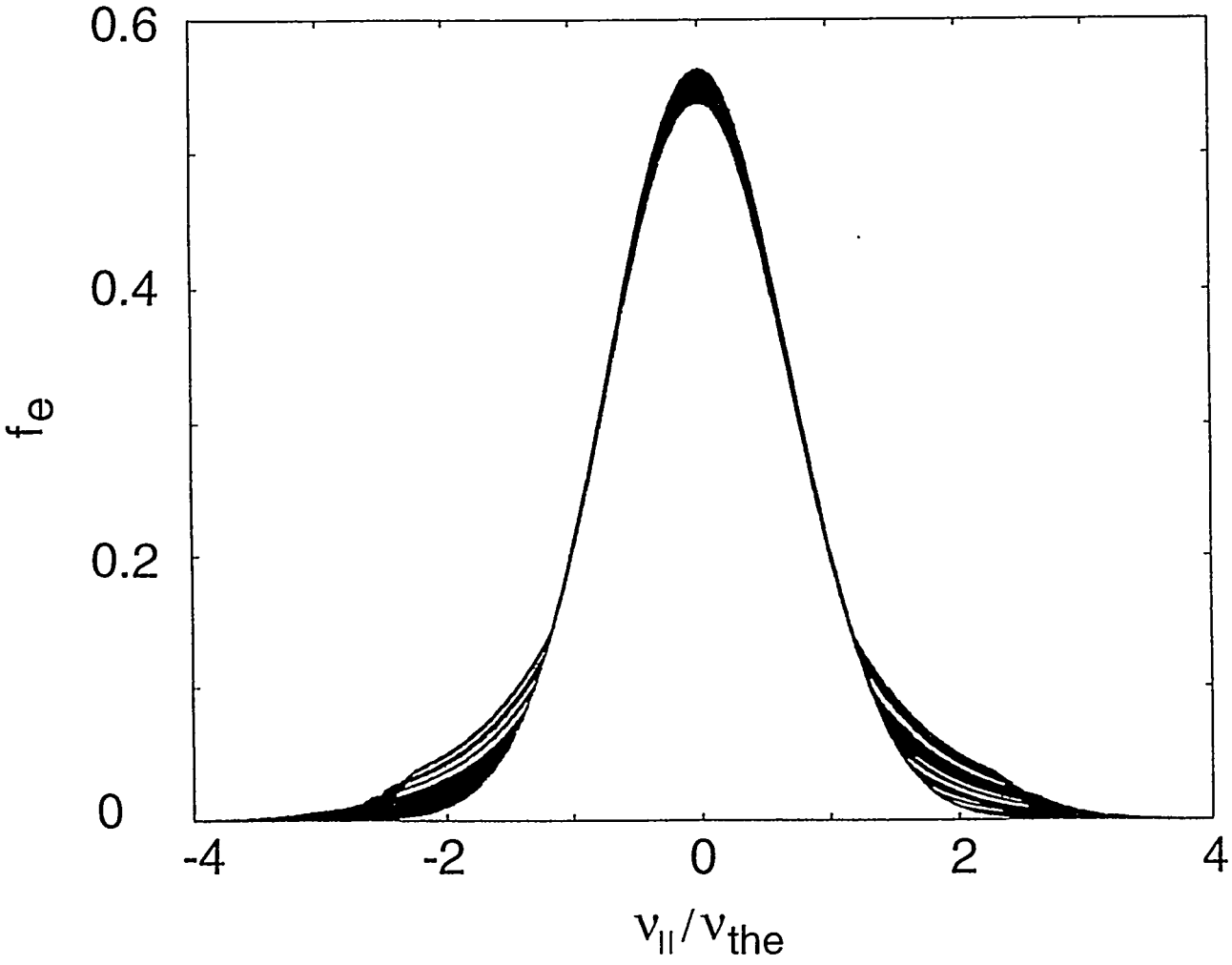


Fig. 7

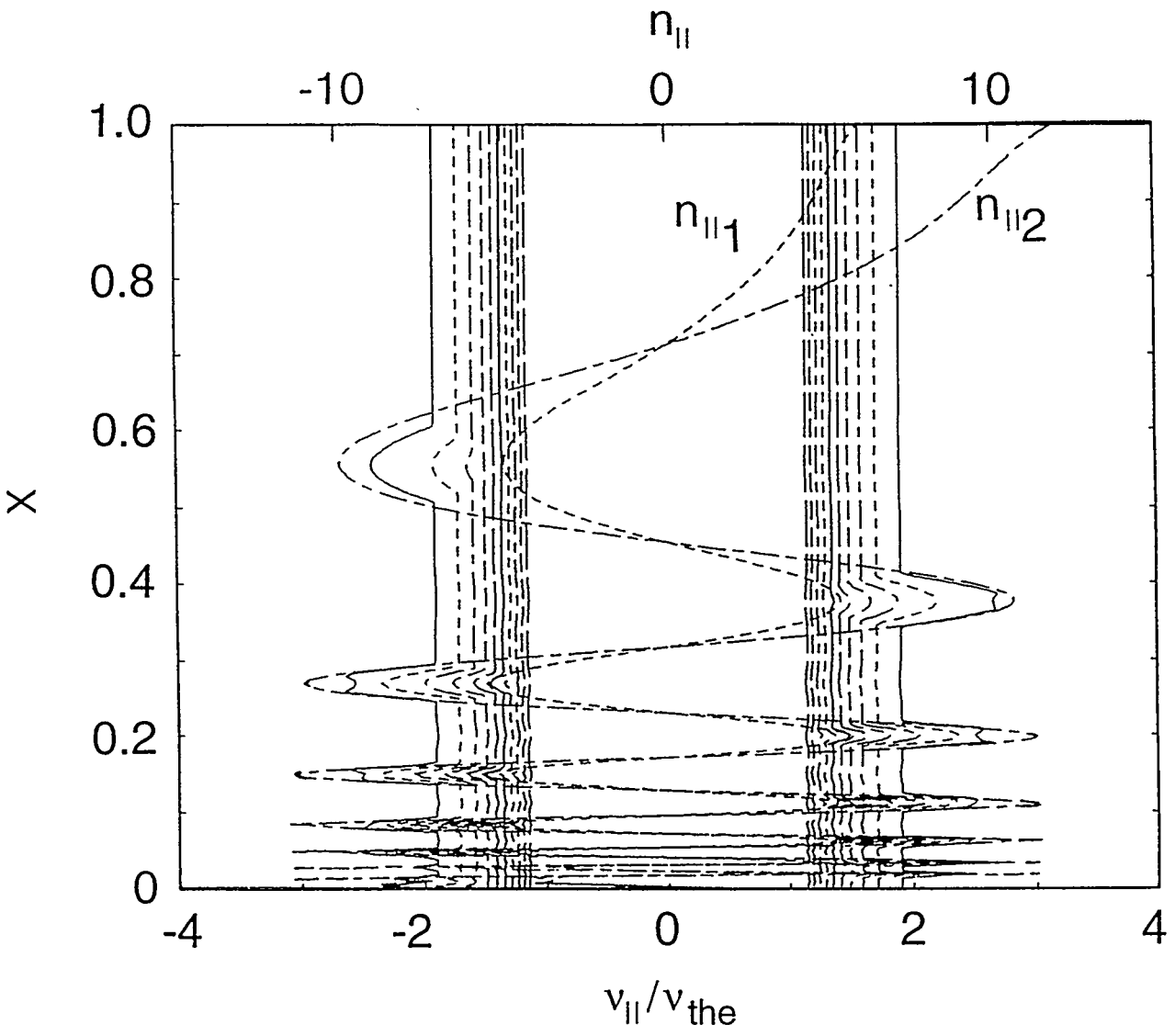


Fig. 8

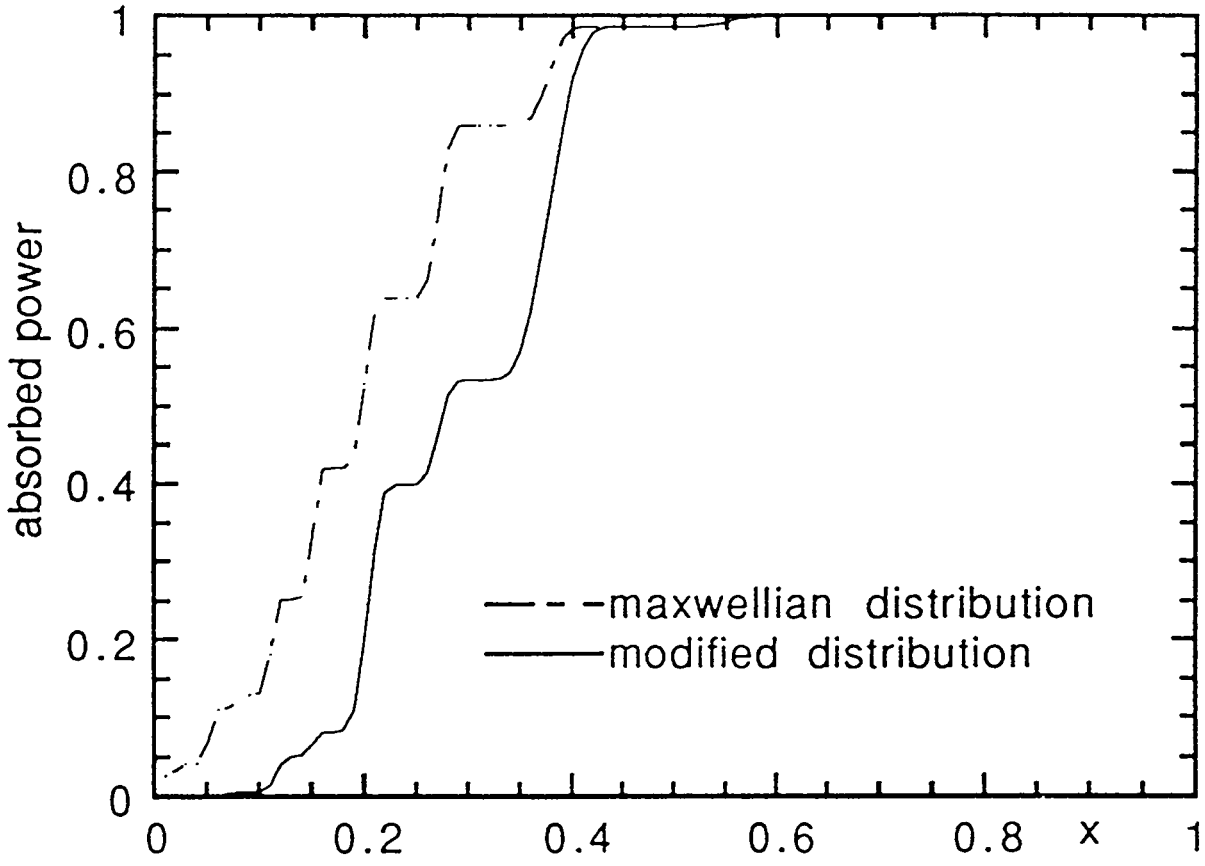
absorbed power
1
0.8
0.6
0.4
0.2
0
0
0.2
0.4
0.6
0.8
x
1
maxwellian distribution
modified distribution

Fig. 9

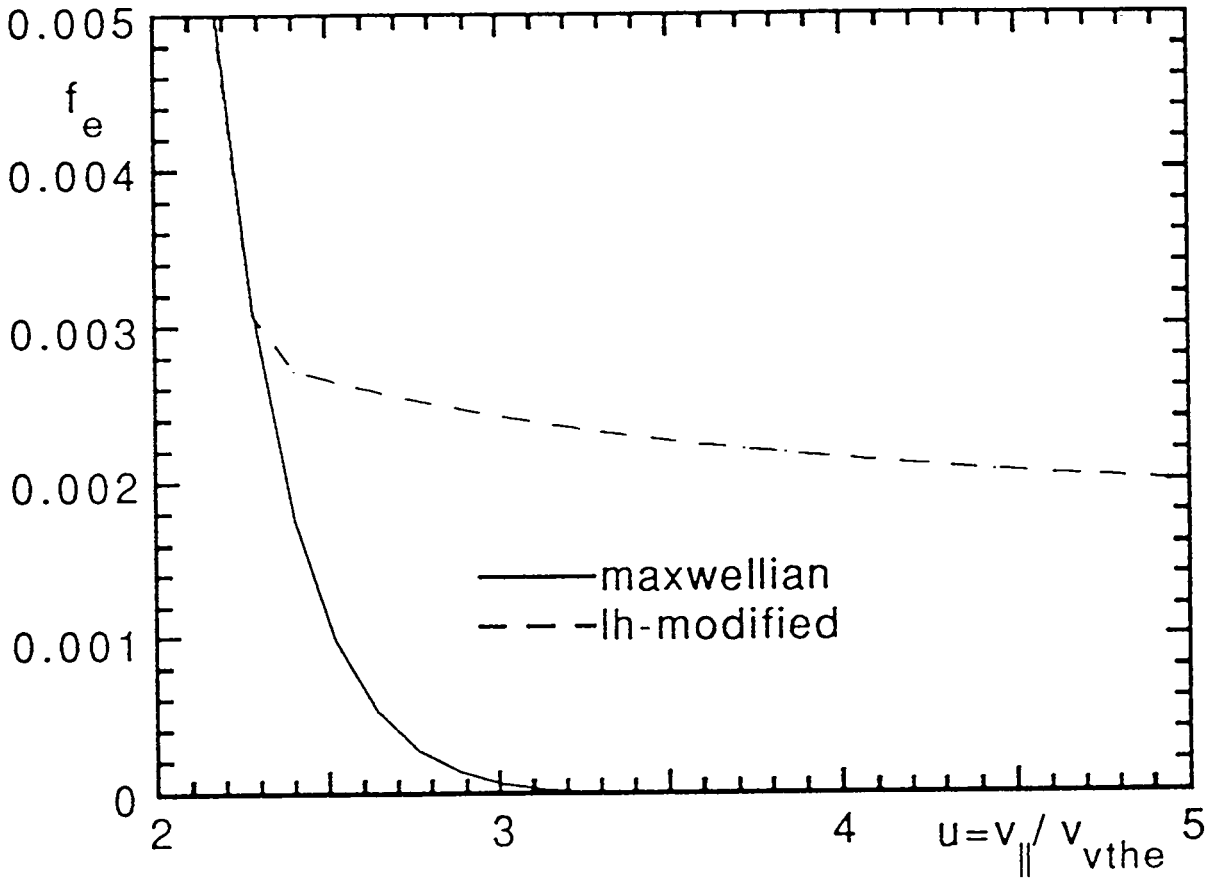
0.005
$f_e$
0.004
0.003
0.002
0.001
0
2
3
4
5
$u=v_{\|}/v_{vthe}$
maxwellian
lh-modified

Fig. 10

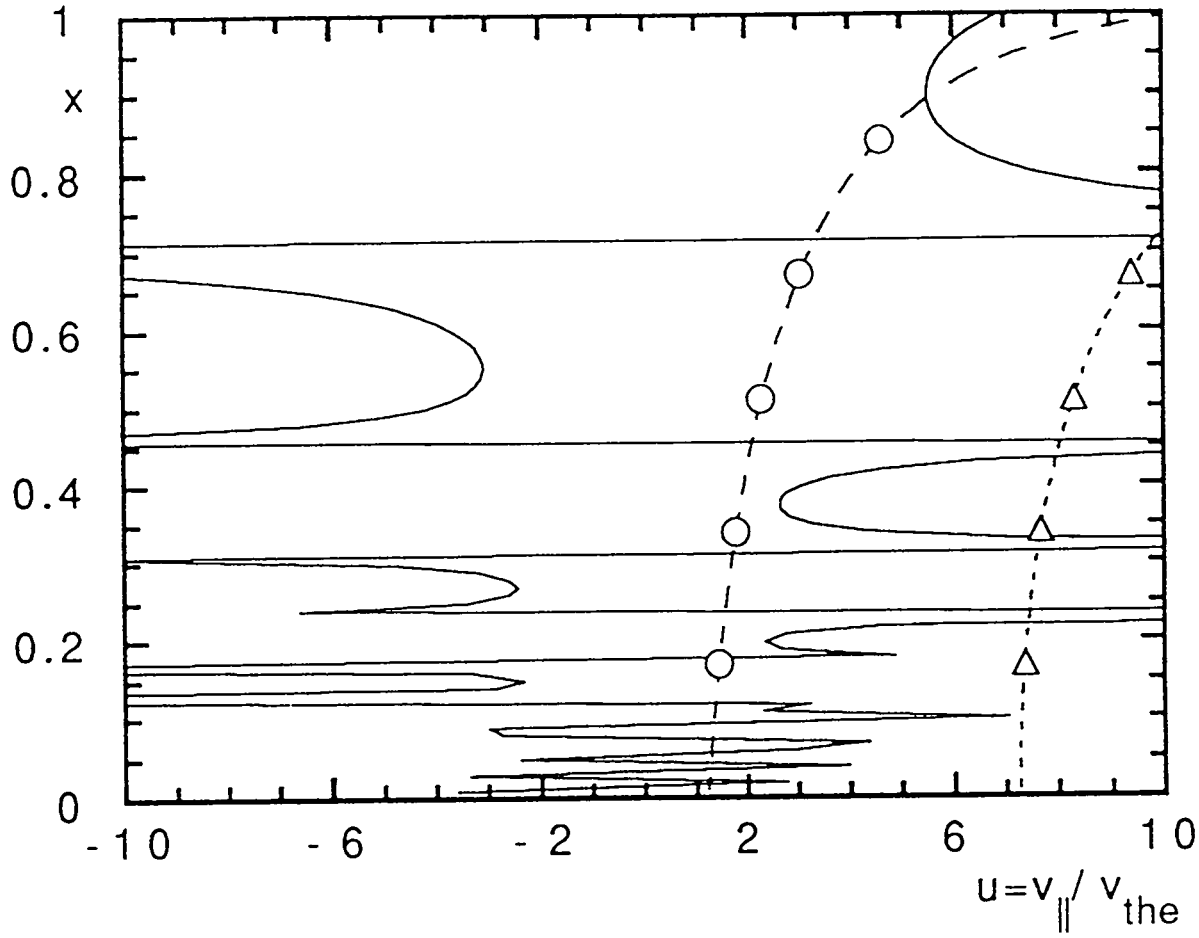


Fig. 11

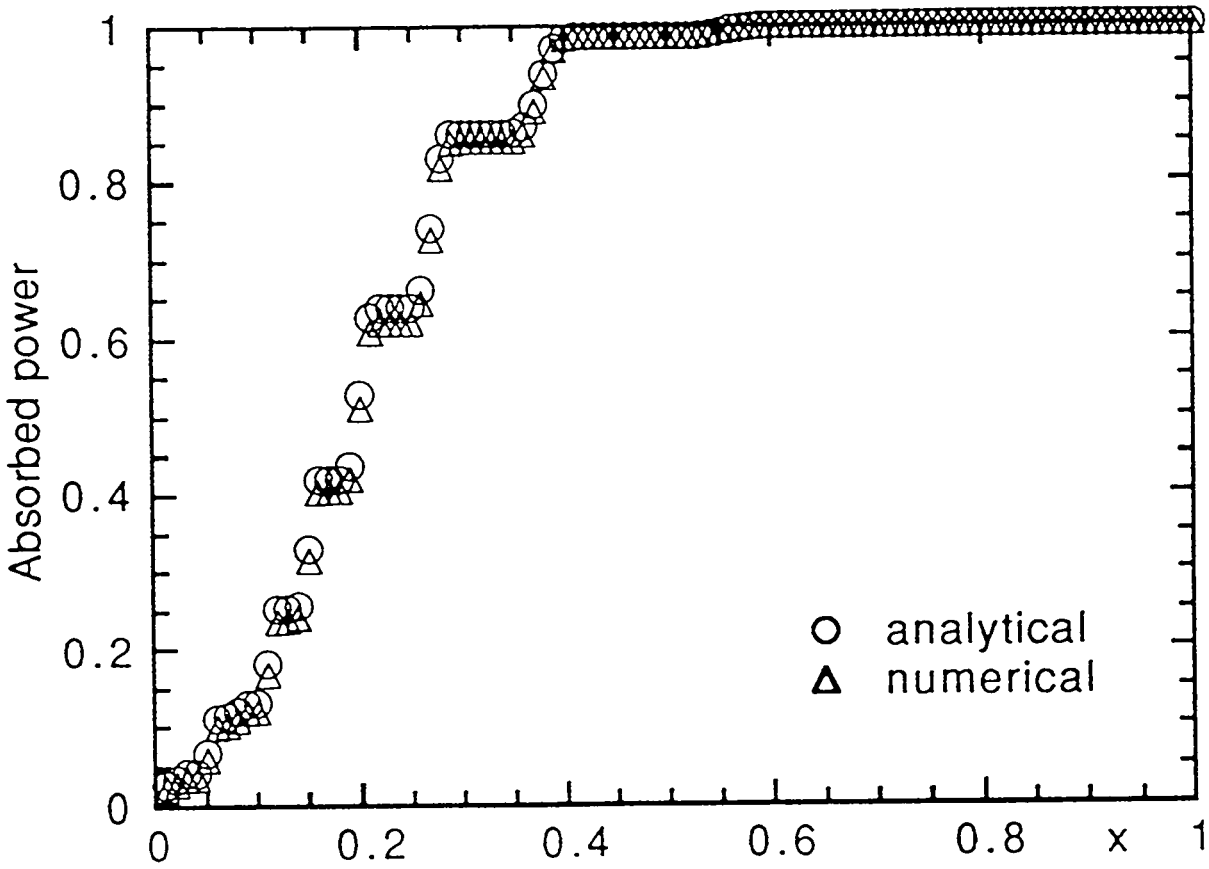
Absorbed power
1
0.8
0.6
0.4
0.2
0
0
0.2
0.4
0.6
0.8
x
1
analytical
numerical

Fig. 12

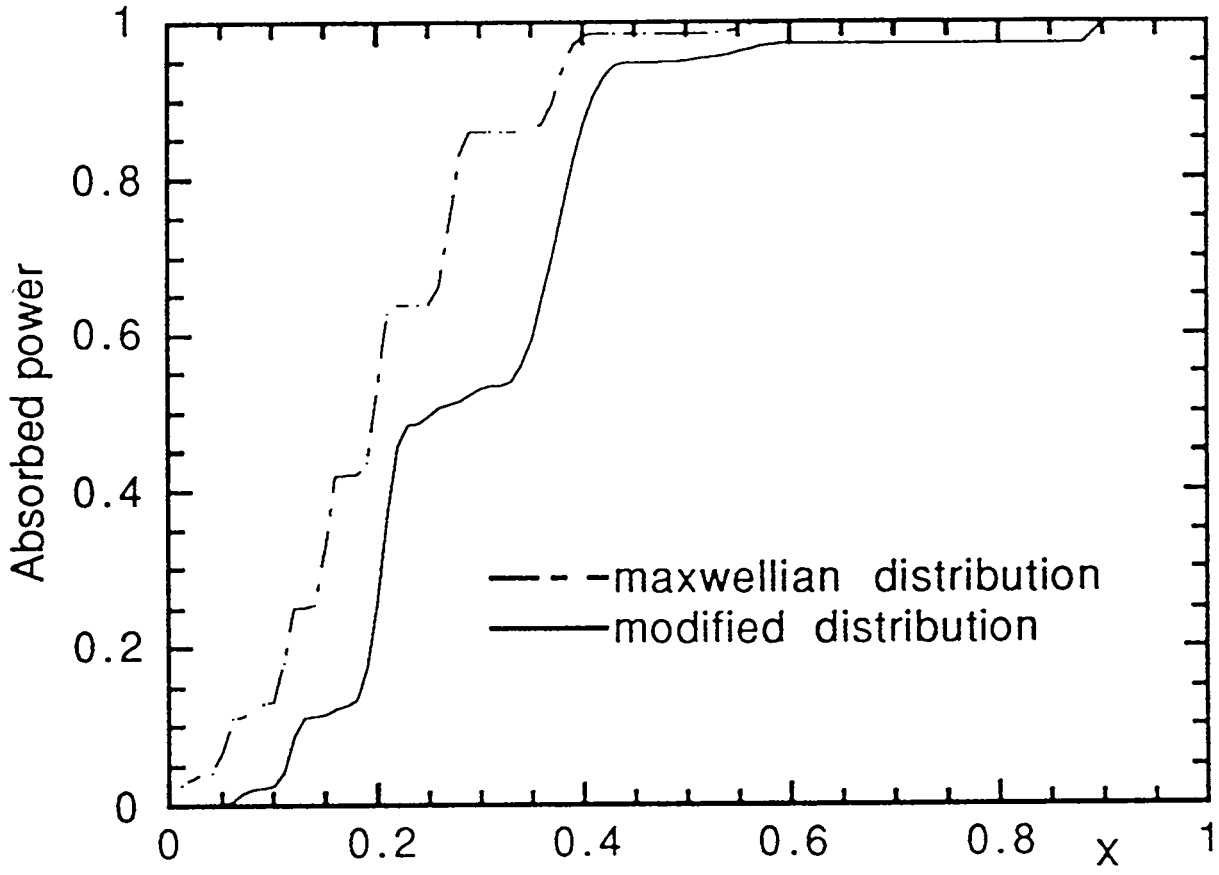
Absorbed power
1
0.8
0.6
0.4
0.2
0
0
0.2
0.4
0.6
0.8
X
1
maxwellian distribution
modified distribution

Fig. 13

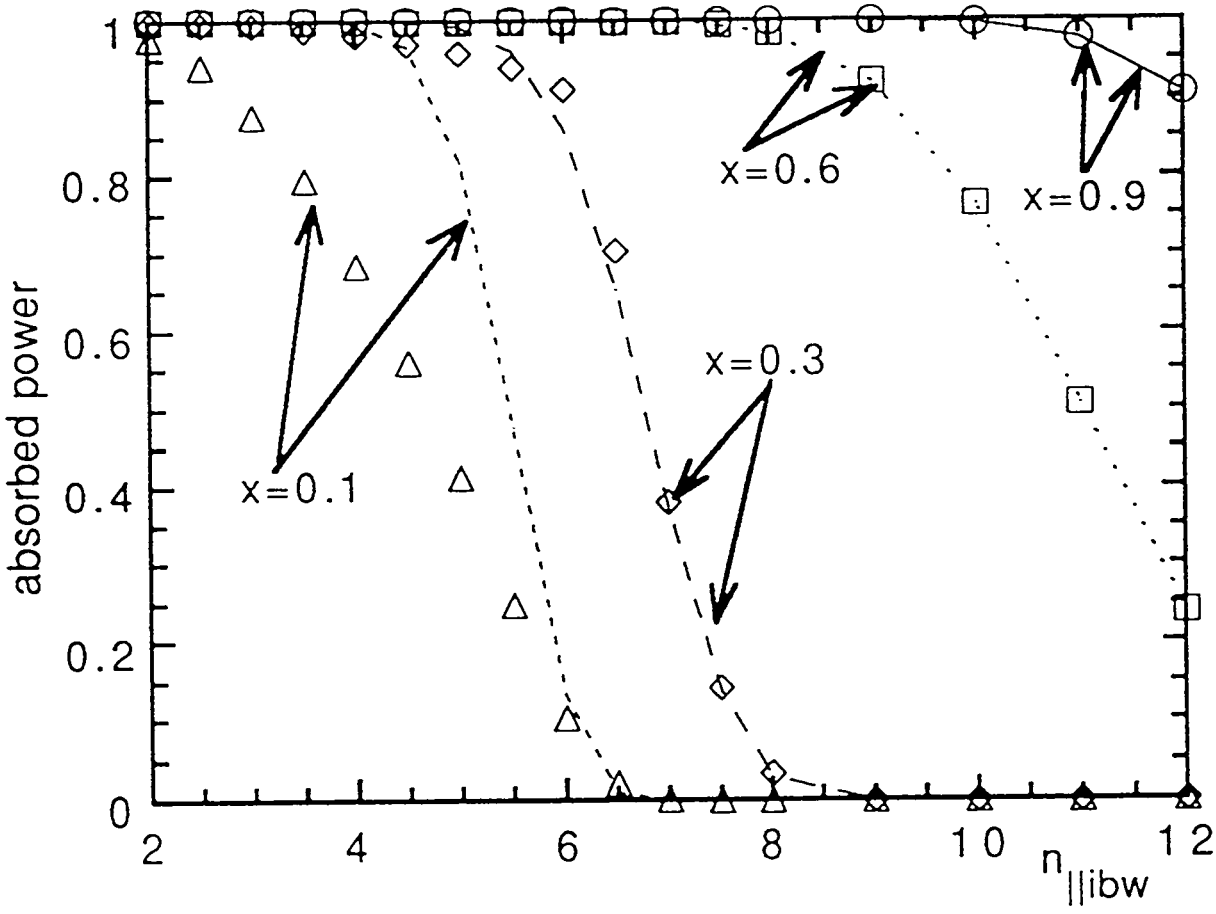


Fig. 14

EXTERNAL DISTRIBUTION IN ADDITION TO UC-420

Dr. F. Paoloni, Univ. of Wollongong, AUSTRALIA
Prof. R.C. Cross, Univ. of Sydney, AUSTRALIA
Plasma Research Lab., Australian Nat. Univ., AUSTRALIA
Prof. I.R. Jones, Flinders Univ, AUSTRALIA
Prof. F. Cap, Inst. for Theoretical Physics, AUSTRIA
Prof. M. Heindler, Institut für Theoretische Physik, AUSTRIA
Prof. M. Goossens, Astronomisch Instituut, BELGIUM
Ecole Royale Militaire, Lab. de Phy. Plasmas, BELGIUM
Commission-European, DG. XII-Fusion Prog., BELGIUM
Prof. R. Boucique, Rijksuniversiteit Gent, BELGIUM
Dr. P.H. Sakanaka, Instituto Fisica, BRAZIL
Prof. Dr. I.C. Nascimento, Instituto Fisica, Sao Paulo, BRAZIL
Instituto Nacional De Pesquisas Espaciais-INPE, BRAZIL
Documents Office, Atomic Energy of Canada Ltd., CANADA
Ms. M. Morin, CCFM/Tokamak de Varennes, CANADA
Dr. M.P. Bachynski, MPB Technologies, Inc., CANADA
Dr. H.M. Skarsgard, Univ. of Saskatchewan, CANADA
Prof. J. Teichmann, Univ. of Montreal, CANADA
Prof. S.R. Sreenivasan, Univ. of Calgary, CANADA
Prof. T.W. Johnston, INRS-Energie, CANADA
Dr. R. Bolton, Centre canadien de fusion magnétique, CANADA
Dr. C.R. James,, Univ. of Alberta, CANADA
Dr. P. Lukác, Komenského Universzita, CZECHO-SLOVAKIA
The Librarian, Culham Laboratory, ENGLAND
Library, R61, Rutherford Appleton Laboratory, ENGLAND
Mrs. S.A. Hutchinson, JET Library, ENGLAND
Dr. S.C. Sharma, Univ. of South Pacific, FIJI ISLANDS
P. Mähönen, Univ. of Helsinki, FINLAND
Prof. M.N. Bussac, Ecole Polytechnique,, FRANCE
C. Mouttet, Lab. de Physique des Milieux Ionisés, FRANCE
J. Radet, CEN/CADARACHE - Bat 506, FRANCE
Prof. E. Economou, Univ. of Crete, GREECE
Ms. C. Rinni, Univ. of Ioannina, GREECE
Preprint Library, Hungarian Academy of Sci., HUNGARY
Dr. B. DasGupta, Saha Inst. of Nuclear Physics, INDIA
Dr. P. Kaw, Inst. for Plasma Research, INDIA
Dr. P. Rosenau, Israel Inst. of Technology, ISRAEL
Librarian, International Center for Theo Physics, ITALY
Miss C. De Palo, Associazione EURATOM-ENEA , ITALY
Dr. G. Grosso, Istituto di Fisica del Plasma, ITALY
Prof. G. Rostangni, Istituto Gas Ionizzati Del Cnr, ITALY
Dr. H. Yamato, Toshiba Res & Devel Center, JAPAN
Prof. I. Kawakami, Hiroshima Univ., JAPAN
Prof. K. Nishikawa, Hiroshima Univ., JAPAN
Librarian, Naka Fusion Research Establishment, JAERI, JAPAN
Director, Japan Atomic Energy Research Inst., JAPAN
Prof. S. Itoh, Kyushu Univ., JAPAN
Research Info. Ctr., National Instit. for Fusion Science, JAPAN
Prof. S. Tanaka, Kyoto Univ., JAPAN
Library, Kyoto Univ., JAPAN
Prof. N. Inoue, Univ. of Tokyo, JAPAN
Secretary, Plasma Section, Electrotechnical Lab., JAPAN
Dr. O. Mitarai, Kumamoto Inst. of Technology, JAPAN
Dr. G.S. Lee, Korea Basic Sci. Ctr., KOREA
J. Hyeon-Sook, Korea Atomic Energy Research Inst., KOREA
D.I. Choi, The Korea Adv. Inst. of Sci. & Tech., KOREA
Prof. B.S. Liley, Univ. of Waikato, NEW ZEALAND
Inst of Physics, Chinese Acad Sci PEOPLE'S REP. OF CHINA
Library, Inst. of Plasma Physics, PEOPLE'S REP. OF CHINA
Tsinghua Univ. Library, PEOPLE'S REPUBLIC OF CHINA
Z. Li, S.W. Inst Physics, PEOPLE'S REPUBLIC OF CHINA
Prof. J.A.C. Cabral, Instituto Superior Tecnico, PORTUGAL
Prof. M.A. Hellberg, Univ. of Natal, S. AFRICA
Prof. D.E. Kim, Pohang Inst. of Sci. & Tech., SO. KOREA
Prof. C.I.E.M.A.T, Fusion Division Library, SPAIN
Dr. L. Stenflo, Univ. of UMEA, SWEDEN
Library, Royal Inst. of Technology, SWEDEN
Prof. H. Wilhelmson, Chalmers Univ. of Tech., SWEDEN
Centre Phys. Des Plasmas, Ecole Polytech, SWITZERLAND
Bibliotheek, Inst. Voor Plasma-Fysica, THE NETHERLANDS
Asst. Prof. Dr. S. Cakir, Middle East Tech. Univ., TURKEY
Dr. V.A. Glukhikh,Sci. Res. Inst. Electrophys.I Apparatus, USSR
Dr. D.D. Ryutov, Siberian Branch of Academy of Sci., USSR
Dr. G.A. Eliseev, I.V. Kurchatov Inst., USSR
Librarian, The Ukr.SSR Academy of Sciences, USSR
Dr. L.M. Kovrizhnykh, Inst. of General Physics, USSR
Kernforschungsanlage GmbH, Zentralbibliothek, W. GERMANY
Bibliothek, Inst. Für Plasmaforschung, W. GERMANY
Prof. K. Schindler, Ruhr-Universität Bochum, W. GERMANY
Dr. F. Wagner, (ASDEX), Max-Planck-Institut, W. GERMANY
Librarian, Max-Planck-Institut, W. GERMANY